

Heavy-Ion Test Results of the Radiation-Hardened Adjustable 0.9A Single Resistor Low Dropout Regulator RH3080MK

September 8th, 2014

Sana Rezgui¹, Rocky Koga², Jeffrey George², Steve Bielat², Todd Owen¹, Todd Bonte¹, and
Robert Dobkin¹

¹Linear Technology, ²The Aerospace Corporation

Acknowledgements

The authors would like to thank David Beebe and Sy Dorlybounxou, from the S-Power Design Product Evaluation Group of Linear Technology for their help with the board design and assembly as well as Steve Bielat and Jeffrey George from The Aerospace Corporation for their assistance with the beam experiments. Special Thanks to the Aerospace Corporation team, mainly David Meshel, and Rocky Koga, for their expediting these experiments.

Executive Summary

This report details the heavy-ion test experiments performed on the RH3080MK at the Lawrence Berkeley National Labs (LBNL). The RH3080MK is a 0.9A Low Dropout linear regulator with a unique architecture featuring a precision current source and voltage follower which allows the output to be programmed to any voltage between zero and 36V, with a single-resistor. The wafer lots are processed to Linear Technology's in house Class S flow to yield circuits usable in stringent military and space applications. Heavy-ions induced SEE (Single Event Effect) experiments included Single Event Transient (SET), Single Event Upset (SEU) and Single Event Latchup (SEL) tests up to an LET of 117.5 MeV.cm²/mg at elevated temperatures (to case temperatures of 100°C). Under heavy-ion irradiations, with various power supply and input biases, as well as load conditions at the op-amp outputs, the RH3080MK showed sensitivities only to SETs. Beam tests confirmed the immunity of this part to SEL and SEU in all test conditions. The measured SET sensitive saturation cross-section is about 9E-4 cm², about 4% of the total die's cross-section, while the SET threshold LET was about 3 MeV.cm²/mg.

The beam data correlated well with previous laser SET data published for this part [4] but not under heavy-ions data [6]. Up to an LET of 58.78 MeV.cm²/mg, the SET pulse widths were shorter in time than 20us, and their delta amplitudes varied between -0.25V and +0.15V with SET shapes similar to the circuit's response to variations in the line or load regulation circuitries. For accurate selection of the circuit peripheral parasitic, we would recommend that the designer simulates his design by injecting SETs at the circuit's inputs/outputs, as wide as the observed SETs in this report. This could be accomplished by the LTSpice tool offered by Linear Technology, as most of the Linear LT parts spice models are offered [7]. That should provide guidance to the designer but the result should be correlated with laser and beam tests as most of the RH and LT parts differ in their process and sometimes in their design as well. The wrong selection of these parasitic can make things worse as they may widen these SETs from tens to hundreds of microseconds, and make it harder on the following circuit to not propagate them.

1. Overview

This report details the heavy-ion test experiments performed on the RH3080MK at the Lawrence Berkeley National Labs (LBNL). The RH3080MK is a 0.9A Low Dropout linear regulator with a unique architecture featuring a precision current source and voltage follower which allows the output to be programmed to any voltage between zero and 36V, with a single-resistor. Multiple regulators can be paralleled to increase total output current and spread heat over a system PC board with no need for heat sinking. The pass transistor collector can be brought out independently of the circuit supply voltage to allow dropout voltage to approach the saturation limit of the pass transistor. A small 2.2 μ F capacitor on the output with an ESR of less than 0.5 Ω is adequate to insure stability. Applications with large output load transients require a larger output capacitor value to minimize output voltage change. Input circuitry insures output safe operating area current limiting and thermal shutdown protection. The rated output current of an RH3080-based part is fixed by internal wire length/resistance. Linear Technology dice element evaluations are based on parts rated for 0.9A output current. The wafer lots are processed to Linear Technology's in house Class S flow to yield circuits usable in stringent military and space applications.

The device is qualified and available in TO3-4 Leads (K) hermetically sealed package. More details are given about this RH-LDO in [1, 2 and 3]. This is a 1.5 μ m technology using exclusively bipolar transistors. The part's block diagram is shown in Fig. 1. The K package designation is given in Fig. 2.

Absolute Maximum Ratings

(Note 1) (All voltages relative to VOUT)

VCONTROL Pin Voltage	40V, -0.3V
IN Pin Voltage	40V, -0.3V
SET Pin Current (Note 6)	10mA
SET Pin Voltage (Relative to OUT, Note 6)	0.3V
Output Short-Circuit Duration	Indefinite
Operating Junction Temperature Range (Notes 2, 10)	-55°C to 125°C
Storage Temperature Range	-65°C to 150°C

Note 1: Stresses beyond those listed under Absolute Maximum Ratings may cause permanent damage to the device. Exposure to any Absolute Maximum Rating condition for extended periods may affect device reliability and lifetime.

Note 2: Unless otherwise specified, all voltages are with respect to VOUT. The RH3080MK DICE is tested and specified under pulse load conditions such that $T_J \approx T_A$.

Note 3: Minimum load current is equivalent to the quiescent current of the part. Since all quiescent and drive current is delivered to the output of the part, the minimum load current is the minimum current required to maintain regulation.

Note 4: Dropout results from either of minimum control voltage, VCONTROL, or minimum input voltage, VIN, both specified with respect to VOUT. These specifications represent the minimum input-to-output differential voltage required to maintain regulation.

Note 5: The VCONTROL pin current is the drive current required for the output transistor. This current tracks output current with roughly a 1:60 ratio. The minimum value is equal to the quiescent current of the device.

Note 6: SET pin is clamped to the output with diodes. These devices only carry current under transient overloads.

Note 7: Adding a small capacitor across the reference current resistor lowers output noise. Adding this capacitor bypasses the resistor shot noise and reference current noise; output noise is then equal to error amplifier noise (see LT3080 data sheet and Application Note AN83).

Note 8: Dice are probe tested at 25°C to the limits shown in Table 1. Except for high current tests, dice are tested under low current conditions which assure full load current specifications when assembled.

Note 9: Dice that are not qualified by Linear Technology with a can sample are guaranteed to meet specifications of Table 1 only. Dice qualified by Linear Technology with a can sample meet specifications in all tables.

Note 10: This IC includes over-temperature protection that is intended to protect the device during momentary overload conditions. Junction temperature exceeds the maximum operating junction temperature when over-temperature protection is active. Continuous operation above the specified maximum operating junction temperature may impair device reliability.

Note 11: Current limit may decrease to zero at input-to-output differential voltages ($V_{IN} - V_{OUT}$) greater than 26V. Operation at voltages for both IN and VCONTROL is allowed up to a maximum of 36V as long as the difference between input and output voltage is below the specified differential ($V_{IN} - V_{OUT}$) voltage. Line and load regulation specifications are not applicable when the device is in current limit.

Note 12: Please refer to LT3080 standard product data sheet for Typical Performance Characteristics, Pin Functions, Applications Information and Typical Applications.

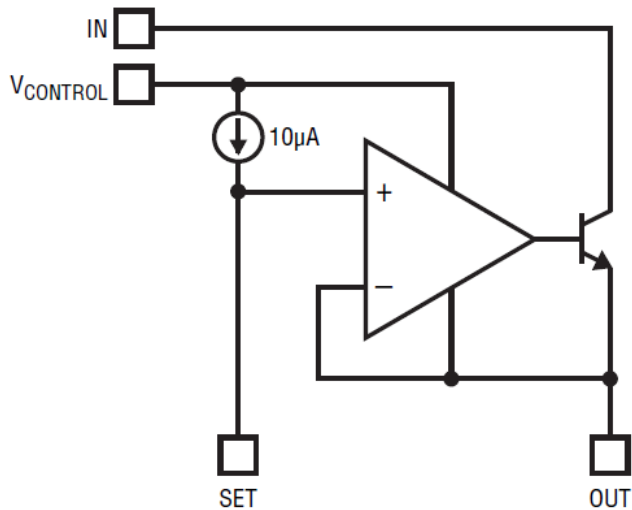


Fig. 1: Block Diagram of the RH3080M DIE

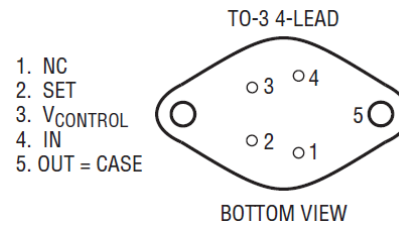


Fig. 2: RH3080M in K Package

Third Party Vendor Availability

Linear Technology partners with third party vendors who assemble and test packaged products with LTC RH Dice inside are listed in Table 1.

Table 1: MS Kennedy and Aeroflex Parts' Availabilities

Part Number	Description	SCD or SMD#
MSK5978RH	0.7A Adjustable, LDO Regulator, Split Bias	-
MSK5977RH	0.9A Adjustable, LDO, Regulator, Split Bias	-
MSK5976RH	1A Adjustable Regulator, Isolated Tab	-
VRG8666	1A Adjustable LDO Regulator, Split Bias	View
MSK5953RH	Dual 1A Adjustable LDO Regulator, Split Bias	-
VRG8667	Dual 1A Adjustable LDO Regulator, Split Bias	View
VRG8668	Dual 1A Adjustable LDO Regulator, Split Bias	View

Table 2 summarizes the parts' features and the electrical test equipment.

Table 2: Test and Part's Information

Generic Part Number	RH3080MK
Package Marking	RH3080MK Fabrication Lot: H0923840.1
Manufacturer	Linear Technology
Quantity tested	2
Dice Dimension	44 mils x75 mils \approx 2.129 mm ²
Part Function	Radiation-Hardened Adjustable 0.9A Single Resistor Low Dropout Regulator
Part Technology	BIPC150 (1.5um)
Package Style	Hermetically sealed TO3-4Leads (K)
Test Equipment	Power supply, oscilloscope, multimeter, and computer
Temperature and Tests	SET, SEU and SEL @ Room Temp. and 100°C

2. Test Setup

Custom SEE boards were built for heavy-ion tests by the Linear Technology team. The RH3080MK parts were tested at LBNL on Apr. 2014 at two different temperatures (at room temperature as well as at 100°C). During the beam runs, we were monitoring the temperature of the adjacent sense transistor (2N3904) to the DUT but not the die temperature (junction temperature). Hence the test engineer needs to account for additional temperature difference between the dice and the sense transistor, which was not measured in vacuum. In-air, both of the case and the sense transistor temperatures were measured to be the same. The temperature difference between the junction of the die and the case is a function of the DUT power dissipation multiplied by the thermal resistance $R_{\text{theta-JC}}(\Theta_{\text{JC}})$. With no heating, the temperature of the adjacent temperature sense transistor (2N3904) to the DUT (or the DUT case) was measured on average at about 25°C. The junction temperature was not measured in vacuum; its calculation is provided in Eq.1. This value was correlated in-air with a thermocouple.

$$T_J = T_C + P_D * \Theta_{\text{JC}} \quad (1)$$

Where: T_J is the junction temperature, T_C the case temperature, P_D the power dissipated in the die and Θ_{JC} the thermal resistance between the die and the case. Note: A relatively small amount of power is dissipated in other components on the board. That is not considered in this calculation.

The calculation of the dissipated power in the die is provided in Eq. 2:

$$P_D = P_{\text{DRIVE}} + P_{\text{OUTPUT}} \dots\dots\dots (2)$$

Where:

P_{DRIVE} is the power dissipation in the Drive Circuit with $P_{\text{DRIVE}} = (V_{\text{CONTROL}} - V_{\text{OUT}}) * (I_{\text{CONTROL}})$.

P_{OUTPUT} is the power in the output transistor with $P_{\text{OUTPUT}} = (V_{\text{IN}} - V_{\text{OUT}}) * (I_{\text{OUT}})$.

The V_{CONTROL} pin current is the drive current required for the output transistor.

This current tracks output current with roughly a 1:60 ratio.

The I_{CONTROL} is equal to $I_{\text{OUT}}/60$. I_{CONTROL} is a function of output current.

Since I_{CONTROL} is negligible compared to I_{OUT} , equation (2) can be simplified as such:

$$P_D = (V_{\text{IN}} - V_{\text{OUT}}) * (I_{\text{OUT}}) \quad (3)$$

Assuming that:

$$T_C = 25^\circ\text{C}; V_{\text{IN}} = 3.3\text{V}; V_{\text{IN}} = V_{\text{CONTROL}} = 3.3\text{V}; V_{\text{OUT}} = 1.5\text{V}; I_{\text{OUT}} = 0.1\text{A} \text{ and } \Theta_{\text{JC}} = 3^\circ\text{C/W [3]},$$

$$\underline{P_D = 180\text{mW and } T_J \approx 25.5^\circ\text{C}}$$

The SEE board contains:

- The DUT (RH3080MK) with open-top (K package de-capped)
- The input (C2) and output (C5) filtering ceramic capacitors with 10uF each
- All capacitors were not populated except for C2, and C5, as they are needed to insure the good stability of the LDO [1]. Although it is recommended to add 0.1uF on the SET pin, C4 was not populated to not filter the true SET events on the SET output.
- The scope termination is set at 1MOhms.
- The 2N3904 bipolar transistor to sense the board's temperature, placed as close as possible to the DUT.

Fig. 3 shows the SEE test board schematics. The picture of this board is given in Fig. 4.

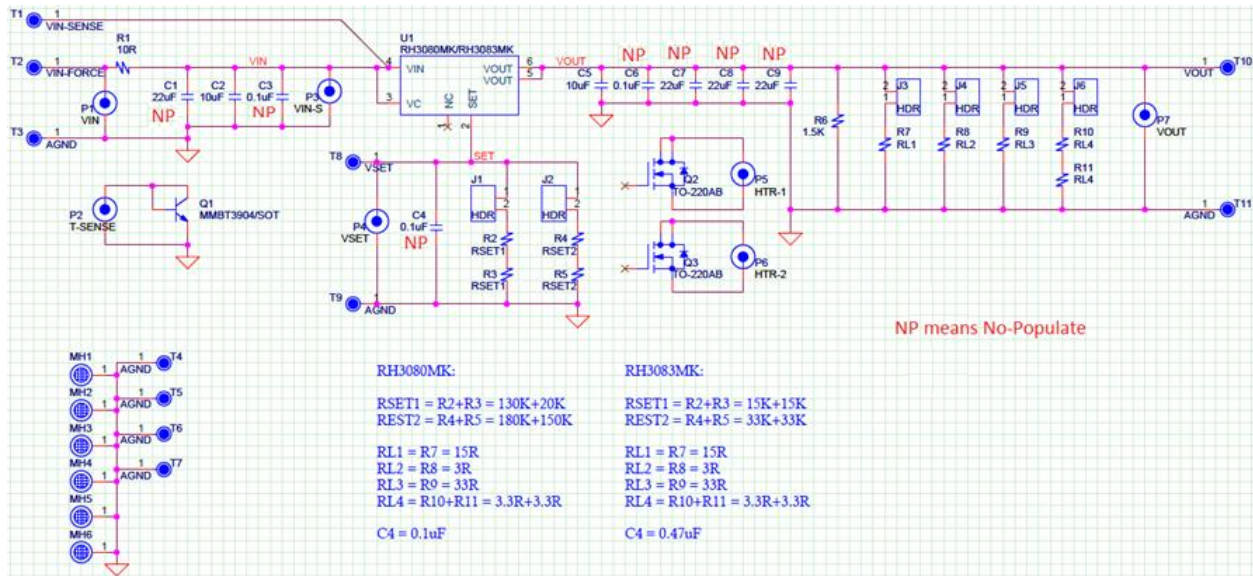


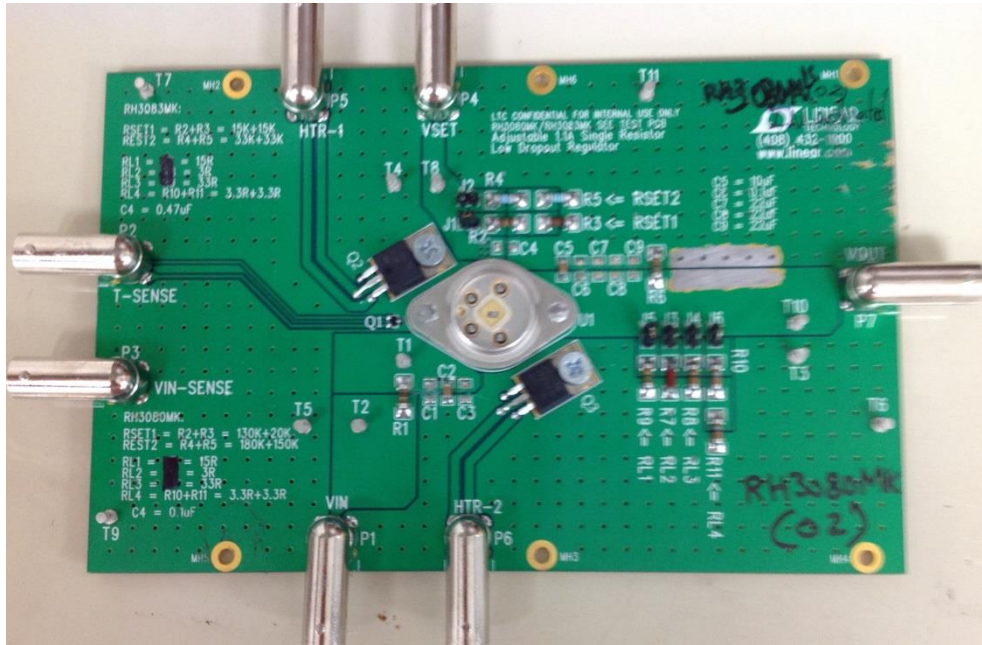
Fig. 3: Block Diagram of the RH3080MK SEE Test Board*

*Note that the same board with changes to some of the passive elements (R_{SET}) was also used to test the 2.8A-RH-LDO RH3083MK to SEEs under heavy-ions. Hence the labeling referred to the RH3083MK part on the board.

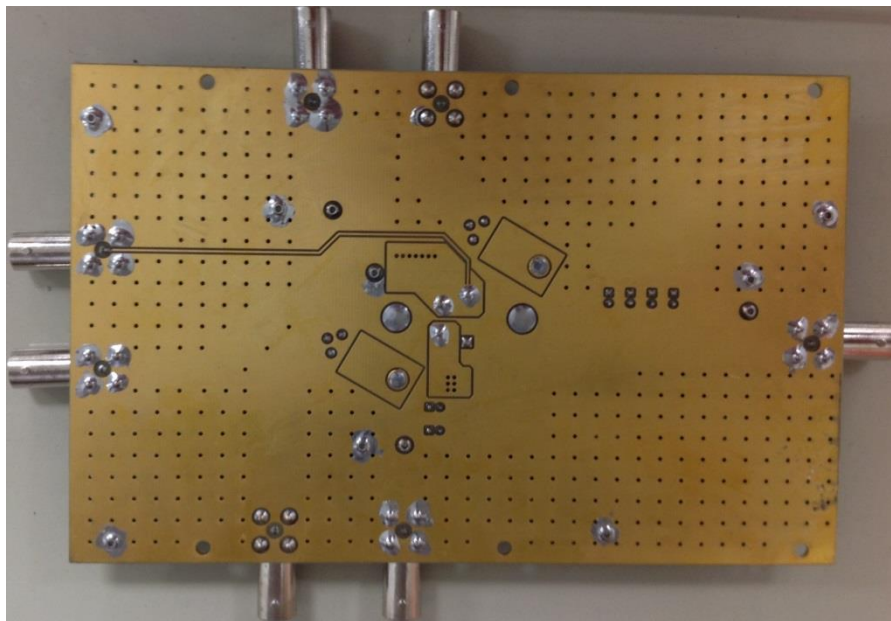
The SEE tests were run with $V_{OUT} = 1.5V$, $I_{OUT} = 0.1A$, $R_{SET} = RH3080MK-R_{SET1} = 150 K\Omega$; $R_{Load} = 15 \Omega$ and with five various input voltage V_{IN} bias conditions, 3.3V, 5V, 10V, 16V and 26V. All radiation test results are provided in Table 5.

In addition, to minimize the distortion of the measured SET pulse-width (PW), the test setup was placed as close as possible to the vacuum chamber. It is connected with two 3 feet long BNC cables to two Agilent power supplies (PS) (N6705B) and to a LeCroy Oscilloscope (Waverunner HRO 66Zi, 600 MHz, 2 GS/s) with extended monitor/cables to view the SET and the V_{OUT} output signals. The first PS supplies the input voltages to the SEE test board and allows the automated logging and storage every 1 ms of the current input supplies (I_{in}), as well as the automation of power-cycles after the detection of a current spike on the input current that exceeds the current limit set by the user. The second PS is used for sensing the voltages of the input power supplies. This was done to avoid any interference from the power supplies that might cause widening of the transients upon the occurrence of an SET.

The SET signal and VOUT output signals were connected each to a scope channel with 3 feet BNC cable (vacuum chamber feed-through) and a scope probe of 11pF. For better accuracy, the equivalent capacitive load of the BNC cable and the scope probe should be calculated and accounted for, as it might affect the SET pulse width and shape. In this case, the cables' capacitive load was about 120pF. The scope was set with 1MOhms termination.



a) Top Side



b) Bottom Side showing the high number of Thermal Vias that were added to dissipate the heat through Conduction in the Heavy-Ion Vacuum Cell

Fig. 4: Photography of the RH3080MK SEE Test Board

3. Heavy-Ion Beam Test Conditions

The selected beam energy is 10MeV/nucleon, which correlates with beam ions delivered at a rate of 7.7 MHz (eq. to a period of 130 ns). During these 130 ns, the ions are generated only within very short pulses that last for 10 ns, as shown in Fig. 5. At every pulse of 10 ns, N number of particles per square centimeter, depending on the flux, will be irradiating the DUT. The calculation of N is provided in Eq. 3:

$$N = \text{Flux} * 130\text{ns} \quad (3)$$

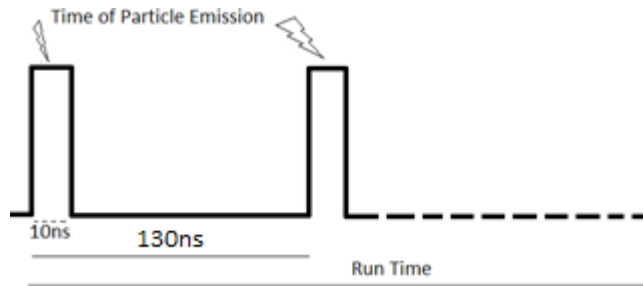


Fig. 5: Particle Emission during a Beam Run at Beam Energy of 10 MeV/nucleon; Emission Frequency = 7.7MHz

For instance if the flux equals 10^4 particles/cm²/second, the probability (N) of having a particle emitted and striking within a defined square centimeter within a random 10ns active period and even during the entire period of 130 ns is 1.30×10^{-3} . Multiply that value by the die area to determine the probability of a particle striking the die; 1.30×10^{-3} particles/cm² * 2.477×10^{-2} cm² = 3.22×10^{-5} . We don't know exactly at what pulse this particle will be irradiating the DUT. The random nature of that emission will change the elapsed time between any two consecutive particles. The higher the beam's frequency or the flux; the higher is the likelihood to have more than one particle hitting the DUT in a very short time (within hundreds of nanoseconds). Indeed, the minimum time that is guaranteed by the facility to separate the occurrences of two particles can be as low as 130 ns but the probability of that happening is very low. To avoid overlapping of events, it is important then that the error-events last less than 130 ns or that the flux is much reduced.

Most importantly, in the case of these analog devices (power, signal conditioning, etc.), some of the DUT's transistors when hit by heavy-ions will cause wide SETs that might last for microseconds. To make sure that the error-rate calculation is accurate, the flux needs to be reduced until there is a consistency in the number of detected errors with the flux for a given ions' fluence. If that's not the case, the part is subject to multiple hits (that might cancel or widen the resulting SET). The test engineer needs to account for these additional effects.

In this case, the beam flux must be set to lower values than 1000p/sec/cm² for two main reasons: 1) avoid cancellation of previous SET effect and 2) avoid increase of the SET pulse width and amplitude when two events overlap. The run fluxes are reported in Table 5. Note that because of the high beam cost, we had exceeded a few times, the maximum flux limit, which led to lower SET cross-sections than the real sensitive cross-section of the part. This was clearly shown at high LETs (Fig. 18) and during the SEL tests, where we needed the fluences to be 10^7 particles/sec.

Also, if the original SET is widened at the DUT output, by the peripheral RC circuits or even the ones used to mitigate it, then the resulting event will dictate the maximum flux to be applied on the DUT. For instance, because of the cabling between the SEE test board and the scope, that adds a minimum capacitive load on the output signal of about 120pF, the final measured SET-PW on the scope can be wider or smaller than the initial SET-PW originating from the DUT output. However, given the cabling requirements (feed-through) at LBNL for vacuum in-beam tests, this minimum capacitive/resistive/inductive load cannot be avoided. For such circuits, it is crucial then to reduce the length, the loading, as much as possible, to avoid reflection of the SET signal through these cables, the beam facility noise effects, etc.

Furthermore, the closer the power supply and the scope is to the test setup, the higher is the likelihood to reduce the noise effects propagating through the beam facility cables and power grids. Ideally, it is advised to have the entire test setup (the power supply along with the SET detection circuit fulfilling the scope function) placed in the vacuum chamber to minimize these effects.

4. Radiation Test Results

Heavy-ions SEE experiments included SET, SEU and SEL tests up to a Linear Energy Transfer (LET) of 117 MeV.cm²/mg at elevated temperatures (to case temperatures of 100°C). In 39 runs, the RH3080MK parts were irradiated under various input bias conditions, a fixed output voltage bias (1.5V), a single resistor (15 Ohms, 1 Watt) equivalent to a 0.1A load, as well as different input supply biases ranging between 3.3 and 26V, as shown in Table 3. As this is a floating LDO, only the differential input to output bias voltage (Vin-Vout) matters. Hence, to speed-up the SEE tests with a few interruptions to the beam chamber vacuum, fixing the output voltage while varying the input voltage is best. The maximum bias was selected to be 26V to meet the datasheet requirement (Note 9 in LT3080 datasheet [2] and Note 11 in RH3080 datasheet [1]), recited below. Table 5 shows the raw data for these runs. Neither SEU nor SEL nor destructive events have been observed during all these tests; all events were transients, with various amplitudes and pulse widths that depended on the LET. The SET cross-sections were independent of the input to output differential voltage in all run heavy-ions beam experiments and used LETs.

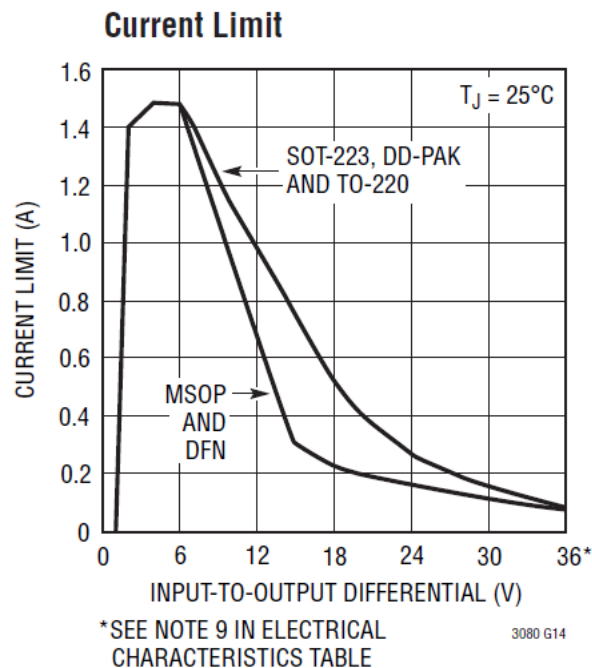


Fig. 7: LT3080 Current Limit, extracted from LT3080 datasheet, Typical Performance Characteristics, page 6*

***LT3080 Online Datasheet** (<http://cds.linear.com/docs/en/datasheet/3080fc.pdf>), page 4:

Note 9 (LT3080, page 4): Current limit may decrease to zero at input-to-output differential voltages (VIN–VOUT) greater than 25V (DFN and MSOP package) or 26V (SOT-223, DD-Pak and T0-220 Package). Operation at voltages for both IN and VCONTROL is allowed up to a maximum of 36V as long as the difference between input and output voltage is below the specified differential (VIN–VOUT) voltage. Line and load regulation specifications are not applicable when the device is in current limit.

Note 11 (RH3080 datasheet, page 3): Current limit may decrease to zero at input-to-output differential voltages (VIN – VOUT) greater than 26V. Operation at voltages for both IN and VCONTROL is allowed up to a maximum of 36V as long as the difference between input and output voltage is below the specified differential (VIN – VOUT) voltage. Line and load regulation specifications are not applicable when the device is in current limit.

Table 3: RH3080MK Bias Test Conditions (Bias, Input, and Output Voltage and Load Currents)

RH-LDO Output Voltage (Vout)	1.5V
Output Load Current (A) / RH-LDO Load Resistor	0.1A / 15 Ohms, 1 Watt
RH-LDO Input Voltage	3.3V, 5V, 10V, 16V, and 26V

Also, the SET-PW on the DUT output is the sum of the prompt effect from the injected SET and the DUT response time to it. The SET amplitude will vary with the injected charge (eq. to LET) and its diffusion in the hit transistor and adjacent transistors to it. Once the hit input transistor has triggered to the ion's deposited charge, and since the circuit response is slower than the ion's hit prompt and diffusion times, the result SET is mostly shaped by the circuit's response times. If hit in the output load circuitry, the SET event will have the shape of the load transient response as shown in Figs. 8 and 9 and if hit in the input part of the circuit, the SET shape will be similar to the line transient response, shown in Fig. 10. Also, all observed SETs started at the SET output and then were shown on the VOUT output signal.

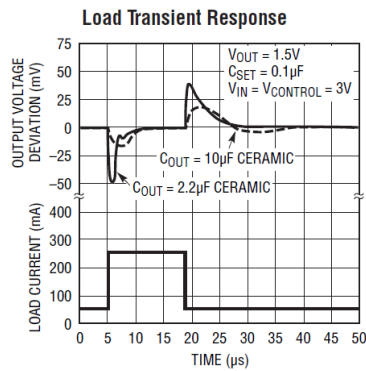


Fig. 8: Load Transient Response vs. Settling Time

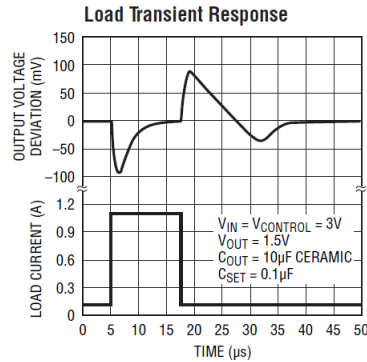


Fig. 9: Load Transient Response vs. Settling Time

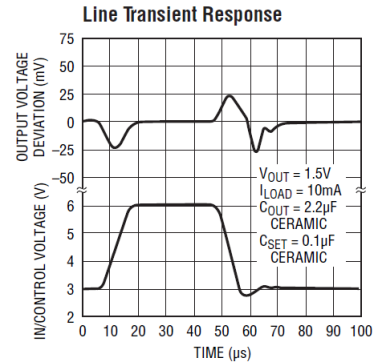


Fig. 10: Line Transient Response vs. Settling Time

Figs. 8, 9 and 10, have been extracted from the Typical Performance Characteristics of the LT3080 datasheet, pg. 6.

For SET detection, the scope was set to trigger on positive and negative SETs as a result of a change in the SET, VOUT, and VIN signals exceeding +/-20 mV (+/-1.3%). The pulse widths were calculated based on these levels as well. Therefore, the reported SET-PW is always smaller than the SET base width (from the time it starts till it ends). All the waveforms were saved during the beam tests and are available to the reader per his/her request.

All of the Single Event Transients started at the SET output with a negative transient pulse (smaller than 44 microseconds in all cases), and remained negative except for a few where a sharp negative transient on the SET signal was followed with a positive pulse, as shown in Fig. 11. Transients on the SET circuitry affected the VOUT output signal in three different ways: 1) positive transient (Fig. 12), 2) negative transient (Fig. 13), and 3) positive and then negative transient on the VOUT signal (Fig. 14). Although wide, most of the transients on the SET signal were small in amplitudes (less than 100mV positive transients and less than 300mV negative transients). On the output VOUT signal, the positive transients were smaller than 150mV and the negative ones smaller than 80mV, both less than +/-10% of the nominal output signal. Additionally, and as shown in Fig. 15, 90% of them were smaller in amplitudes than +/-5% (+/-75mV) of the output VOUT signal. Similar SET amplitudes and widths to the beam observed SETs were shown in [4, 5], during laser tests.

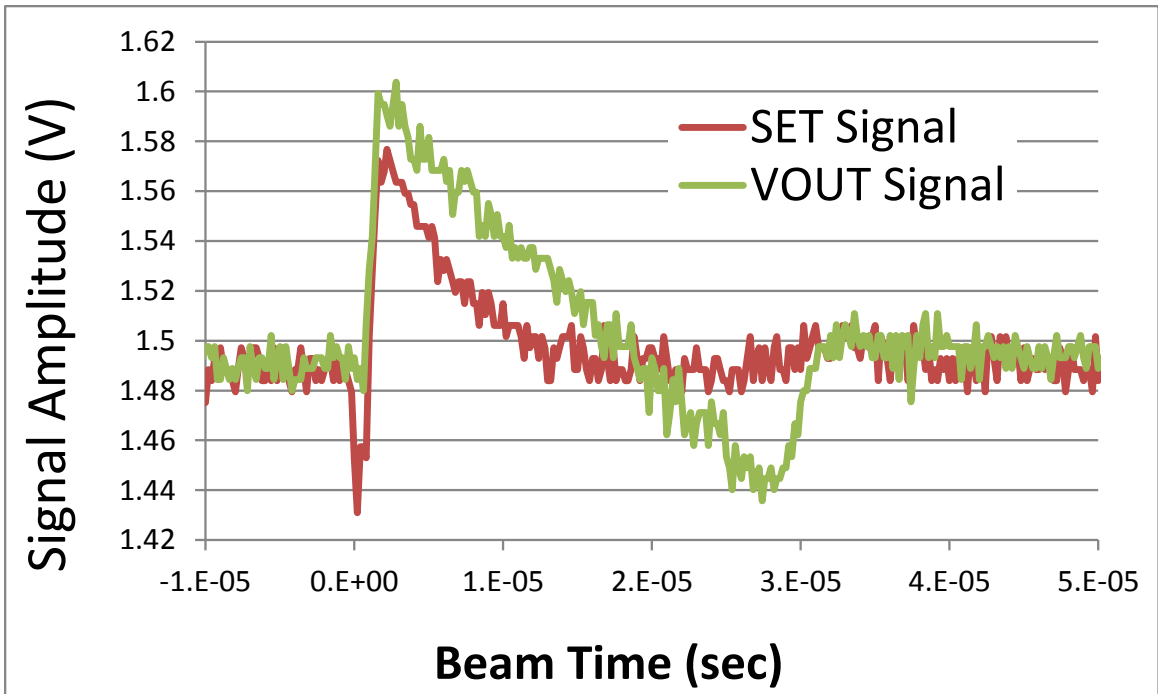


Fig. 11: Negative and Positive Transient Pulse on the SET signal vs. Beam Time

Run 121, Waveform 82

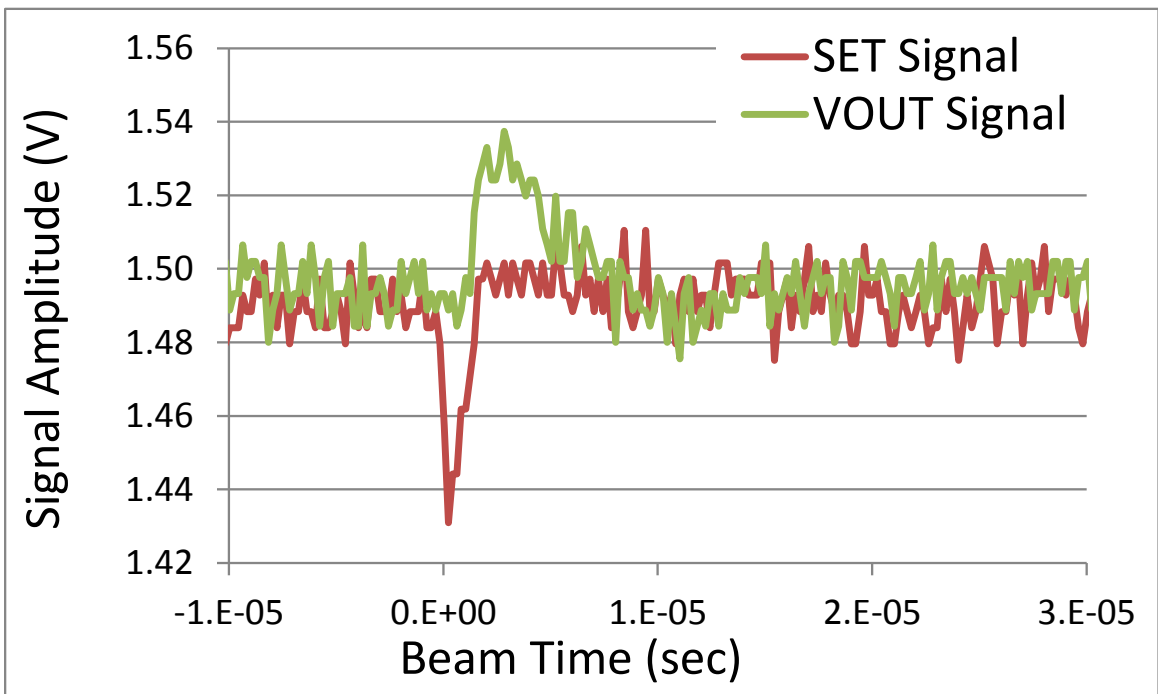


Fig. 12: Positive Transient Pulse on the VOUT Output Signal vs. Beam Time

Run 121, Waveform 5

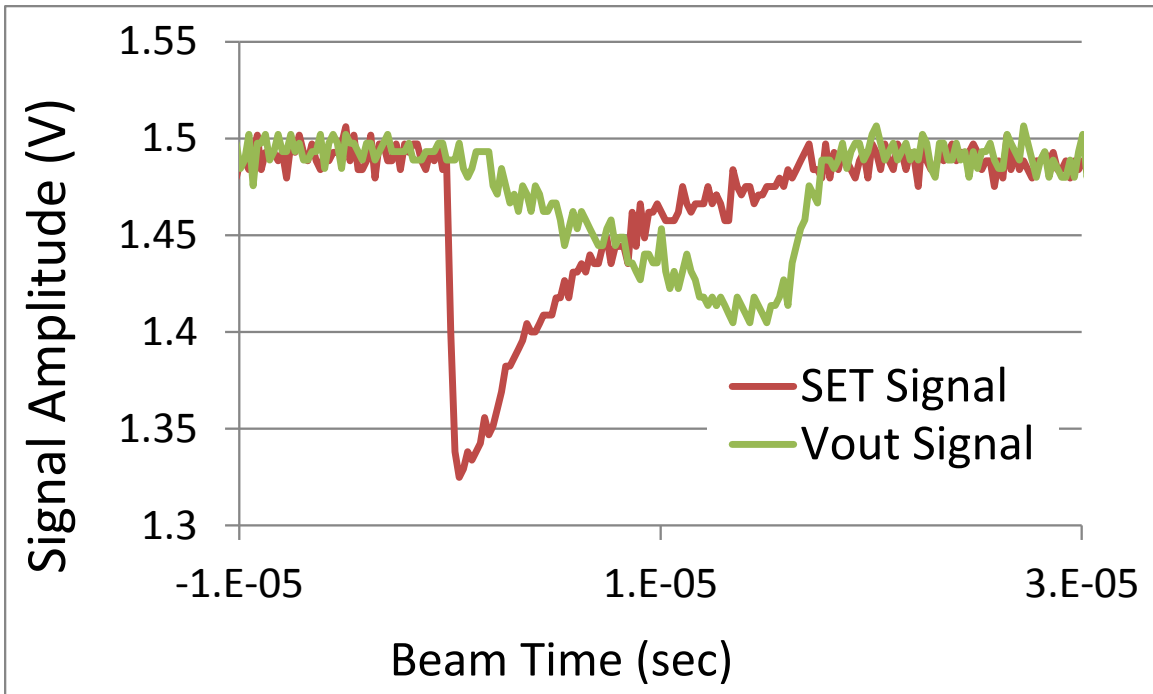


Fig. 13: Negative Transient Pulse on the VOUT Output Signal vs. Beam Time

Run 121, Waveform 9

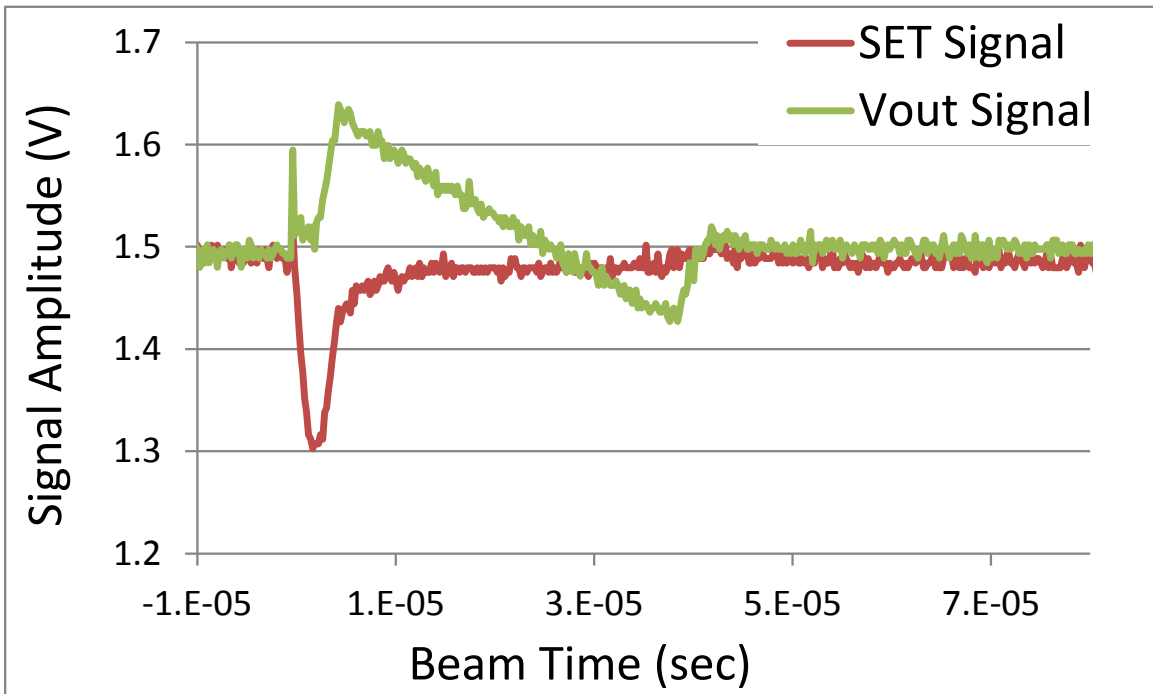


Fig. 14: Positive and then Negative Transient Pulse on the VOUT Output Signal vs. Beam Time;

Run 121, Waveform 13

Finally, Figs. 15 and 16 show that the cumulative distributions with the SET amplitudes and widths, respectively. Fig. 17 shows the SET amplitudes versus the SET pulse-widths.

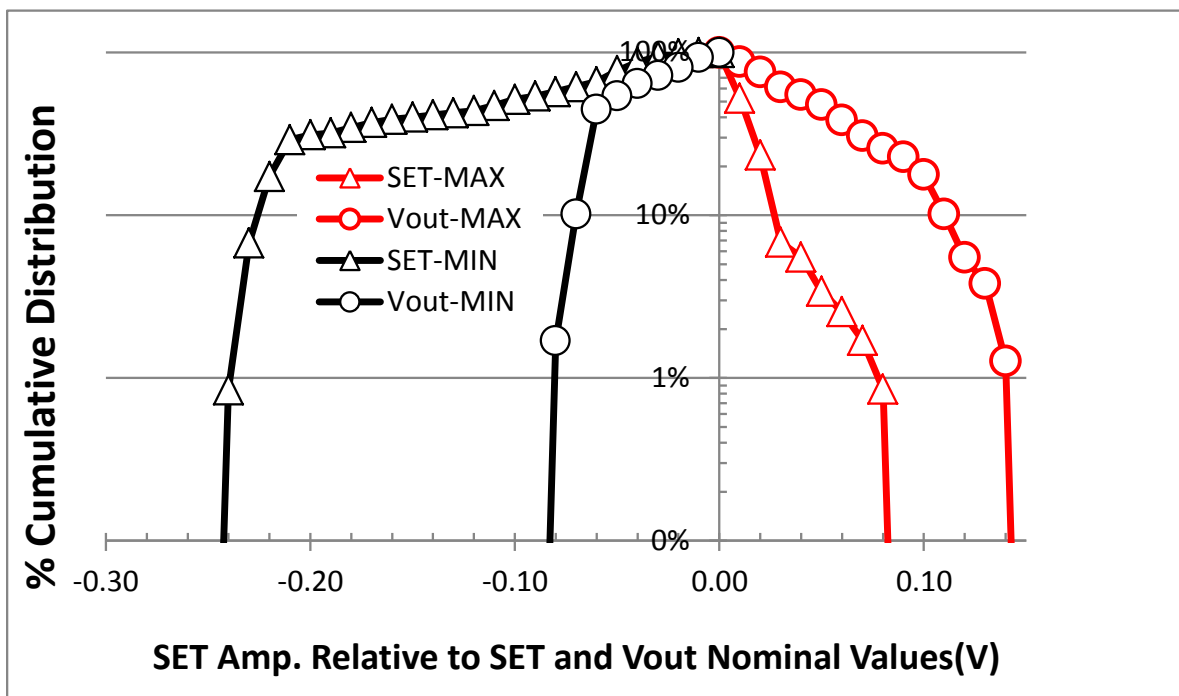


Fig. 15: % Cumulative Distributions vs. SET Pulse-Amplitudes
 Runs#121, 156, $V_{in}=26V$; $V_{out}=1.5V$; $I_{out}=0.1A$; Room Temp.; Xenon Ions with $LET=58.78 \text{ MeV}\cdot\text{cm}^2/\text{mg}$

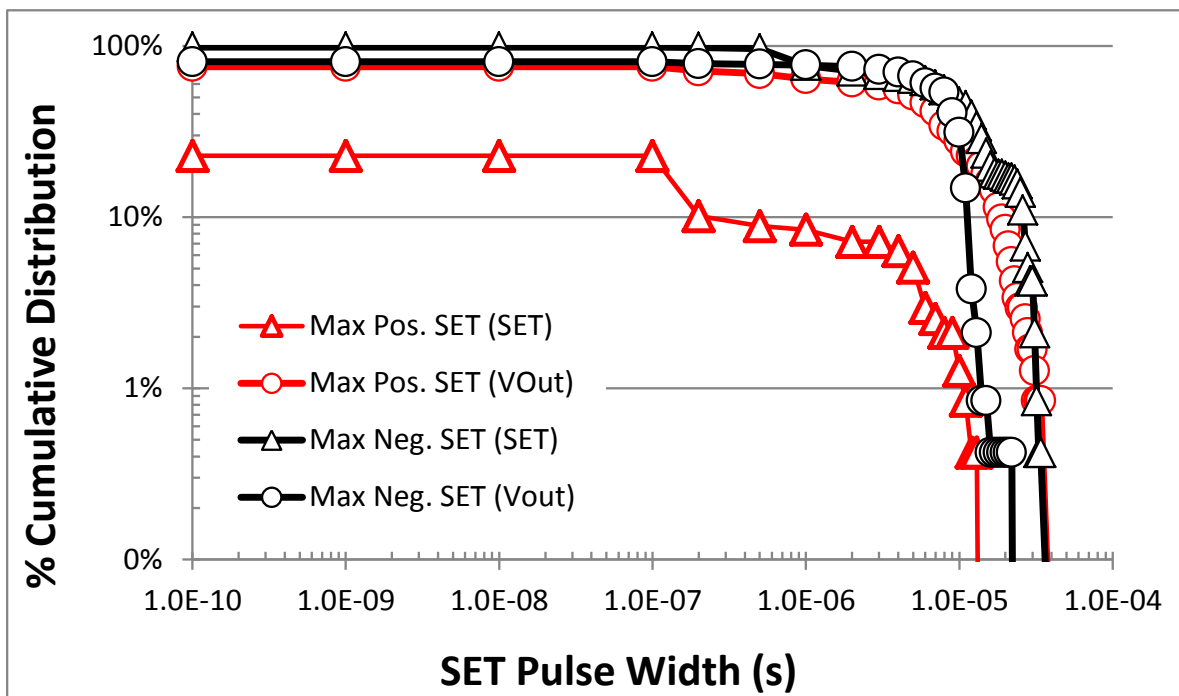


Fig. 16: % Cumulative Distributions vs. SET Pulse-Widths
 Runs#121, 156, $V_{in}=26V$; $V_{out}=1.5V$; $I_{out}=0.1A$; Room Temp.; Xenon Ions with $LET=58.78 \text{ MeV}\cdot\text{cm}^2/\text{mg}$

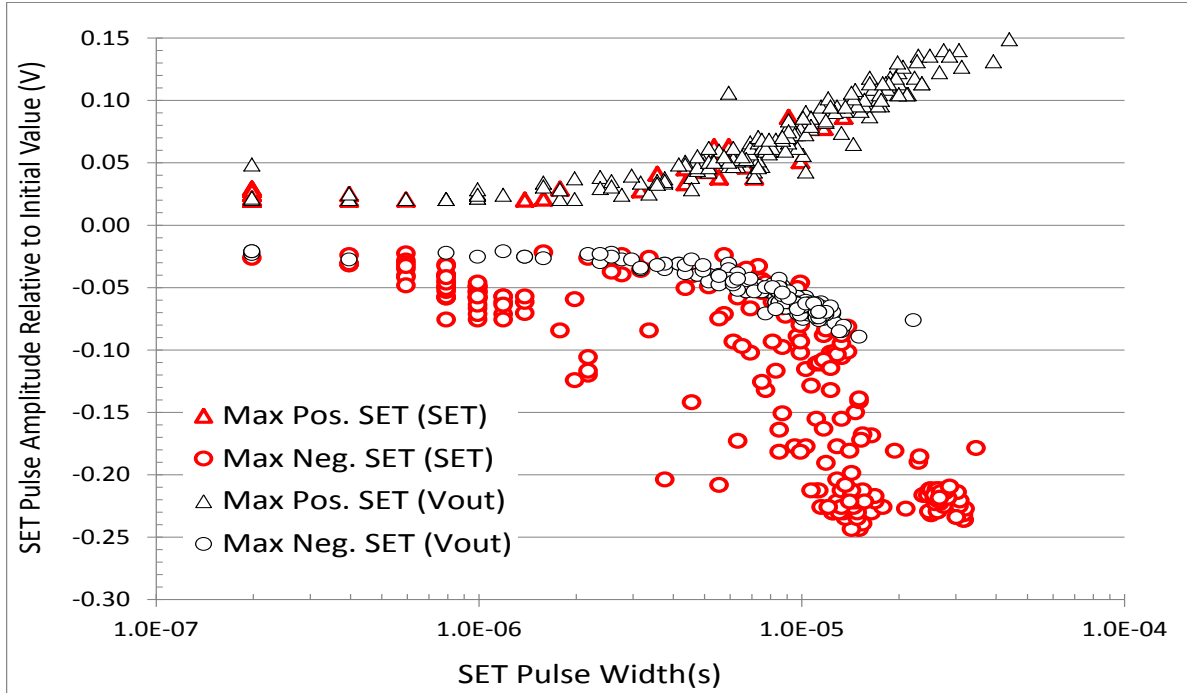


Fig. 17: % SET Pulse-Amplitudes vs. SET Pulse-Widths
 Runs#121, 156, Vin=26V; Vout=1.5V; Iout=0.1A; Room Temp.; Xenon Ions with LET=58.78 MeV.cm²/mg

1) *Input Voltage Supply Effects On the SET Pulse-Amplitudes and Pulse Widths and Cross-Sections*

The beam data showed almost no dependence on the differential input to output voltage supply for the SET Amplitudes and Widths as well as LETs. For complete SET pulse widths and amplitudes dependences on the LETs and Bias conditions, see Appendix A.

Fig. 18 shows the SET cross-sections at different input biases and the fitting Weibull curves that customers can use to determine the RH3080MK orbital error rates in their space flight designs. In Table 4 are provided the Weibull parameters for their calculations, as demonstrated in Eq. 4. Note that if SET pulse amplitudes within 5% of the output signal can be ignored in their designs then the resulting orbital error-rates will be negligible as 90% of these SETs can be ignored.

Table 4: Weibull Parameters Used for the RH3080MK SEE Cross-Section and the Calculation of the Error Rates

L ₀ (MeV / mg-cm ²)	W (MeV / mg-cm ²)	S	σ ₀ (cm ²)
2.4	20	1	9E-4

$$\sigma = \sigma_0 \left[1 - e^{-((L-L_0)/W)^S} \right] \quad (4)$$

In summary, under heavy-ion irradiations, and at the various input bias conditions (Table 3), the RH3080MK showed sensitivities only to SETs. The measured underlying SET sensitive cross-section (all events added) is about 9E-4 cm² (about 4% of the physical die cross-section), while the threshold LET is about 3 MeV.cm²/mg.

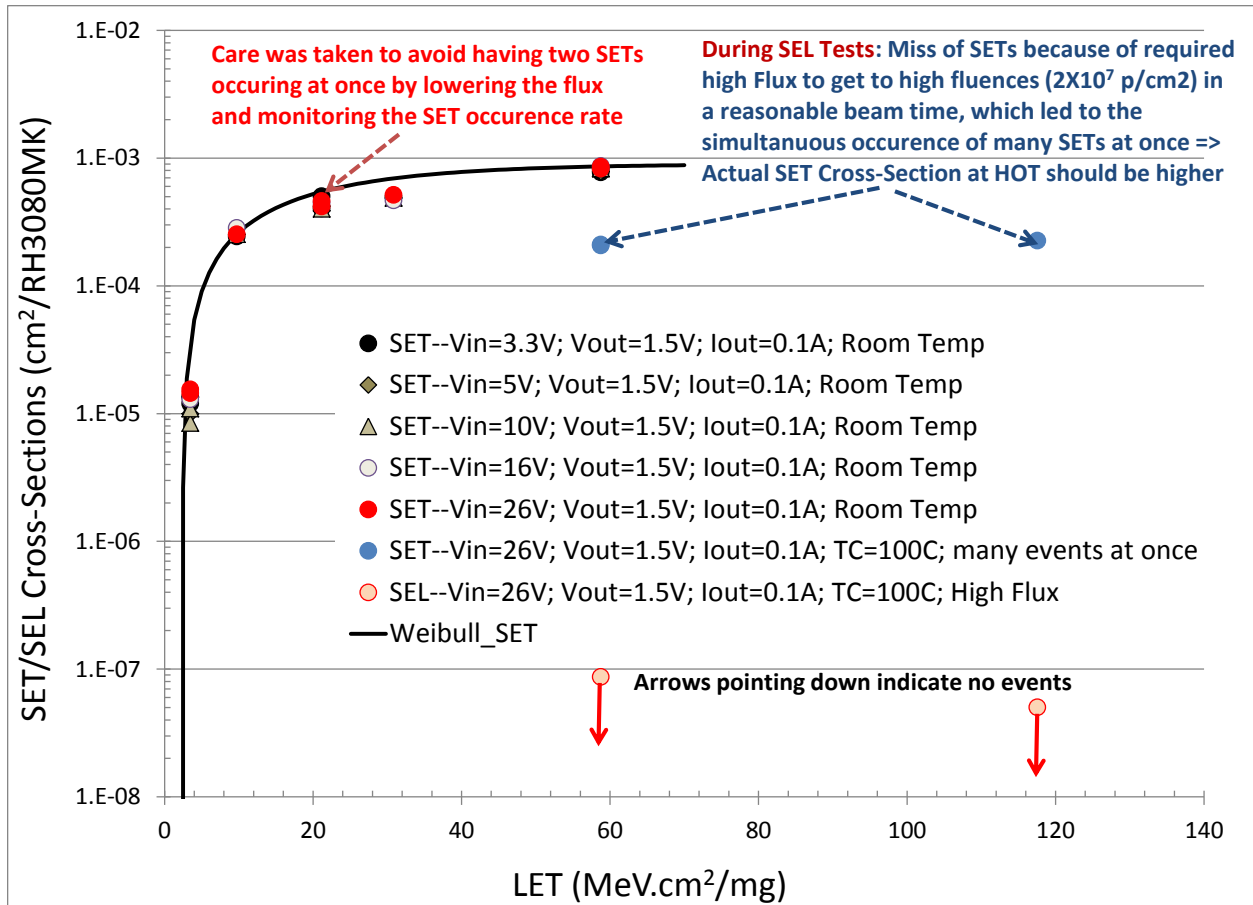


Fig. 18: Measured SET and SEL Cross-Sections vs. LET, showing:

- 1) the RH3080MK immunity to Destructive Events including SELs
- 2) the non-dependence of SET Cross-Sections on the input to output differential voltage

2) *LET Effects on the SET Pulse Widths and Amplitudes*

As expected, Figs. 18 and 19 show that the SET pulse-widths and amplitudes increase with heavy-ion LETs. In addition, except for the width of the negative transient pulses on the SET signal, which still varied with the collected charge, all other SET amplitudes and widths seem to almost saturate above an LET of 9.74 MeV.cm²/mg (Argon ions). On the other hand, the measured negative transient pulse-width on the SET signal with Copper LETs (21.17 MeV.cm²/mg) were lower than with Krypton LETs (30.86 MeV.cm²/mg). This may be due to the high fluxes that were applied during the Copper runs, leading to the summation of two SET pulse-widths at once.

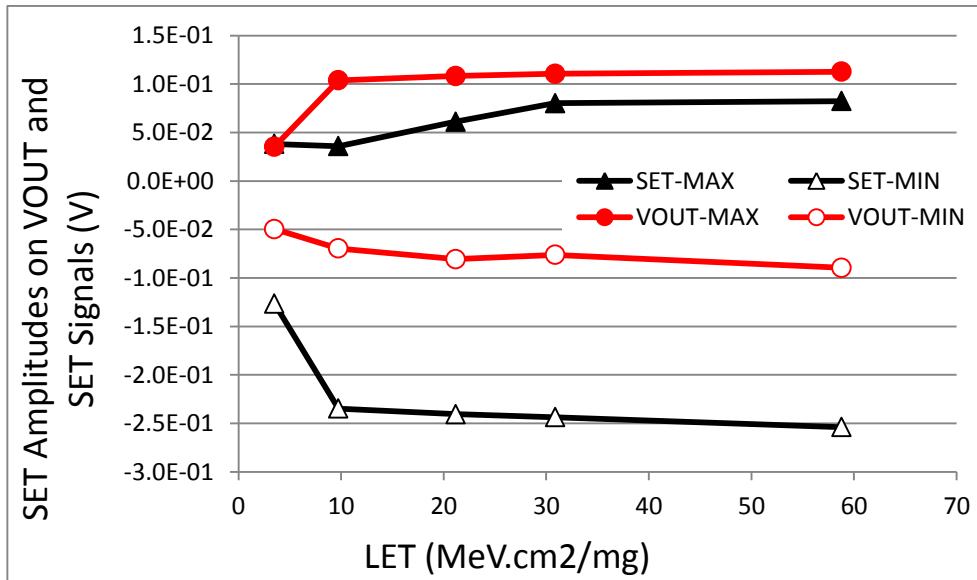


Fig. 18: % SET Maximum Pulse-Amplitudes vs. Linear Energy Transfer (LET)
 Runs#123, 128, 133, 138, 143, 149, 152 and 155; Vin=10V; Vout=1.5V; Iout=0.1A; Room Temp.

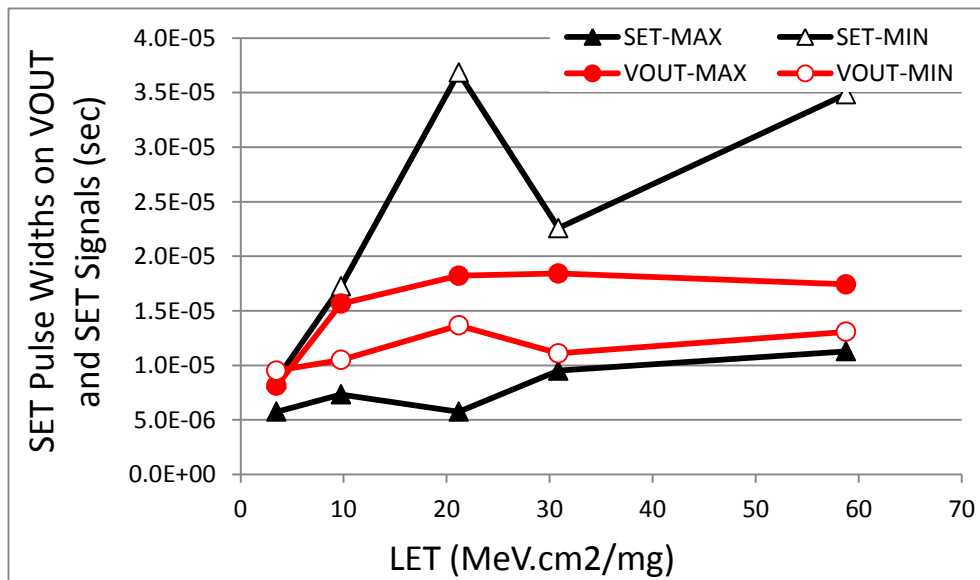


Fig. 19: % SET Maximum Pulse-Widths vs. Linear Energy Transfer (LET)
 Runs#123, 128, 133, 138, 143, 149, 152 and 155; Vin=26V; Vout=1.5V; Iout=0.1A; Room Temp.

2) *SEL Immunity at Hot (100°C) (at 26V Input Voltage)*

At high temperature (100°C) at the DUT case, the test results (red circles in Fig. 20) showed immunity to SELs up to an LET of 117.5 MeV.cm²/mg. SET cross-sections at hot are shown in blue circles. The SEL tests were run at input voltage equal to 26V, output voltage of 1.5V and load current of 100mA.

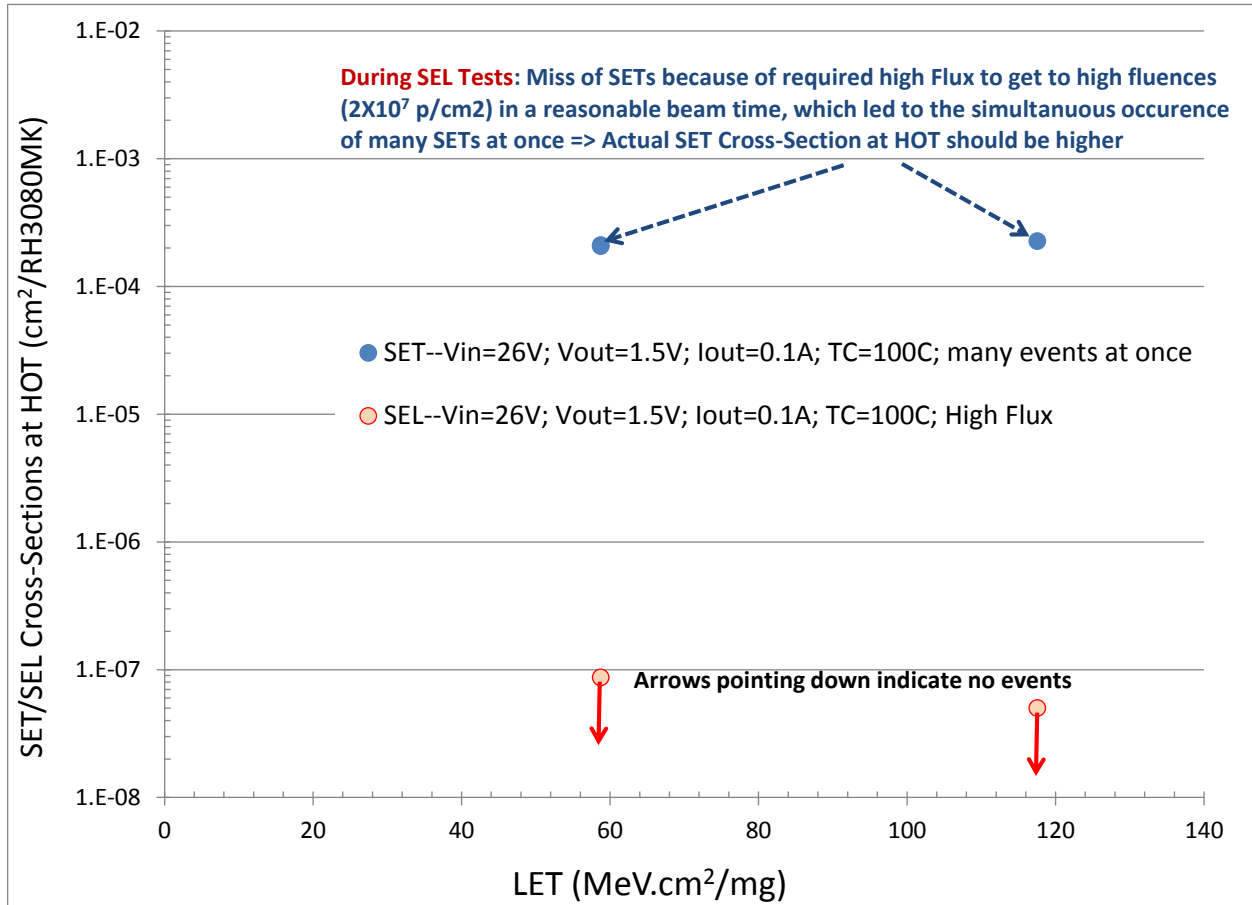


Fig. 20: Measured SEL Cross-Sections vs. LET, showing the RH3080MK immunity to Destructive Events including SELs

Arrows pointing down are indication of no observed SETs up to that fluence at tested LET

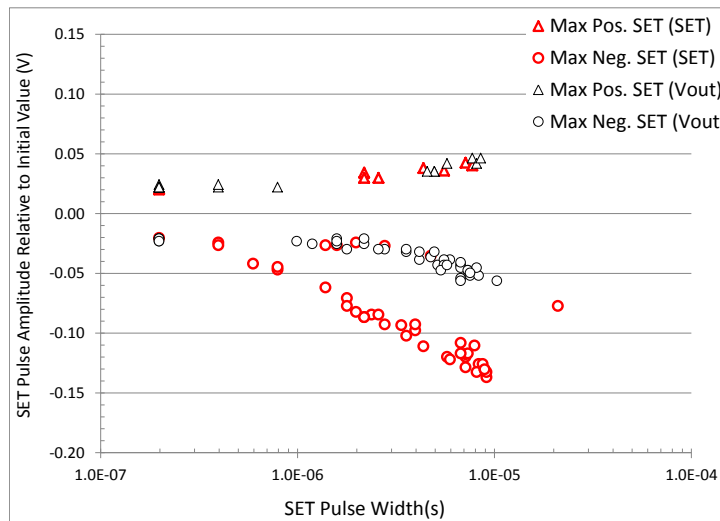
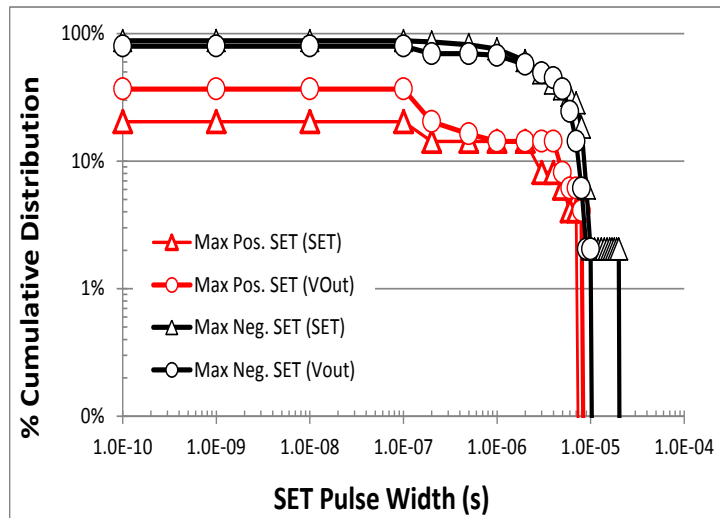
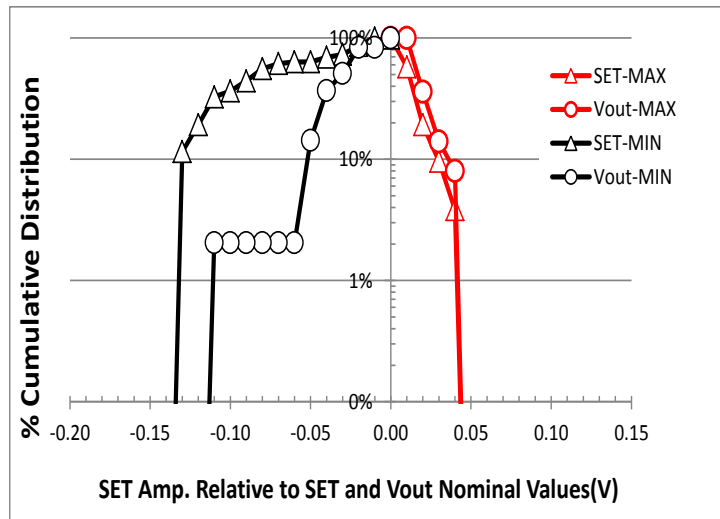
References:

- [1] RH3080M DataSheet: <http://www.linear.com/product/RH3080MK>
- [2] LT3080 Datasheet: <http://www.linear.com/product/LT3080>
- [3] RH3080M Spec.: http://cds.linear.com/docs/en/spec-notice/RH3080MK_DIE_CAN_SAM_05-08-5246_DICE_SPEC_REV__C.pdf
- [4] NASA-GSFC, Jonathan Pellish, Single Event Transient Testing of RH3080 Laser Test Report, June 2006.
- [5] NASA-GSFC, Michael Campola, Dakai Chen, Sana Rezgui, Single Event Transient Testing of RH3080 Laser Test Report, February 2013.
- [6] NASA-GSFC, Dakai Chen, Paul Musil, Single Event Transient Testing of MSK5978RH Heavy-Ions Test Report, August 2012.
- [7] LTSpice: <http://www.linear.com/designtools/software/#LTSpice>

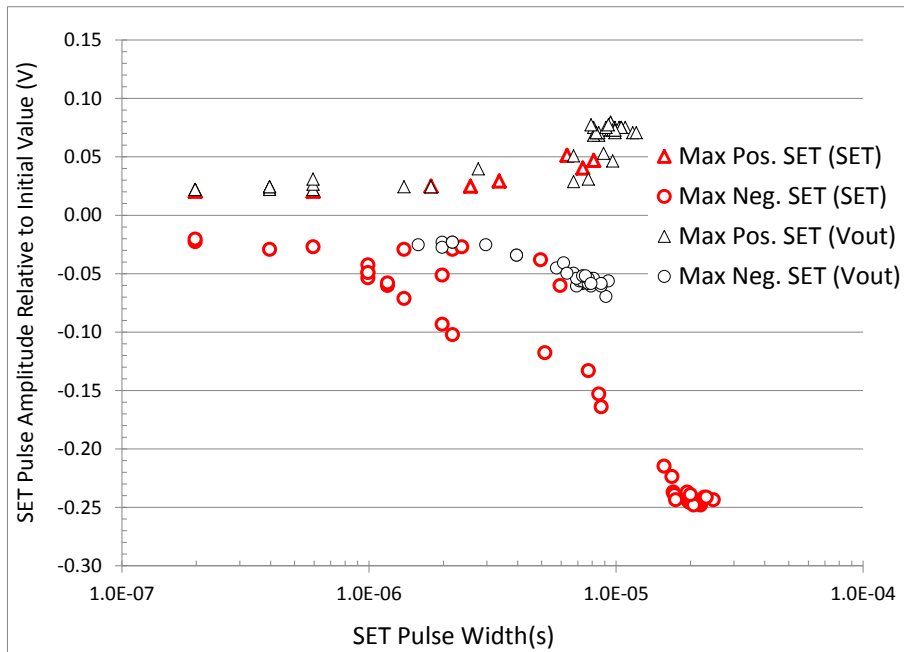
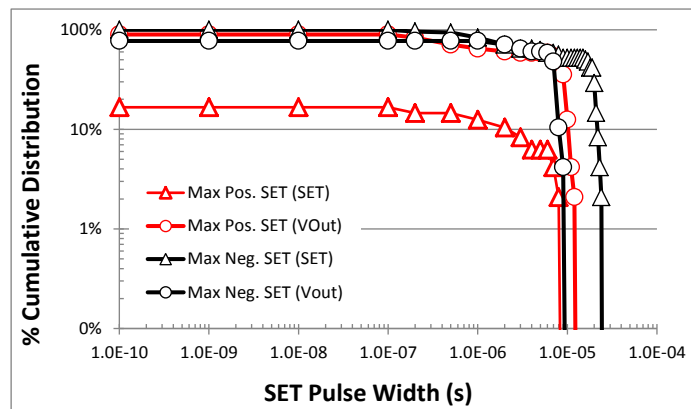
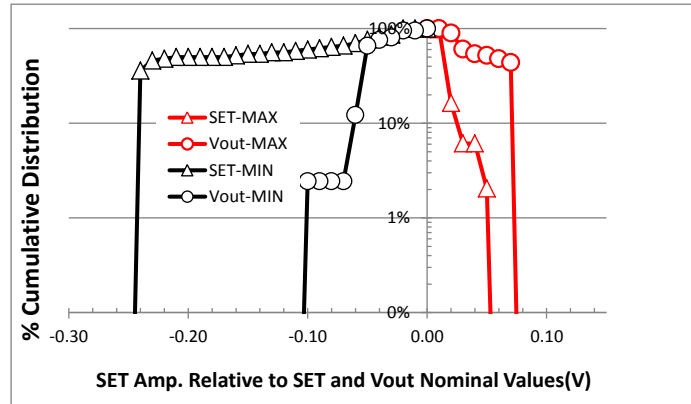
Appendix A.: SET Distributions in Pulse Widths and Amplitudes per Bias Conditions

1. $V_{in}=3.3V$; $V_{out}=1.5V$; $I_{out}=0.1A$; Room Temp.; Neon Ions; $LET=3.49 \text{ MeV.cm}^2/\text{mg}$ (Runs 145, 147)
2. $V_{in}=3.3V$; $V_{out}=1.5V$; $I_{out}=0.1A$; Room Temp.; Argon Ions; $LET=9.74 \text{ MeV.cm}^2/\text{mg}$ (Runs 136)
3. $V_{in}=3.3V$; $V_{out}=1.5V$; $I_{out}=0.1A$; Room Temp.; Copper Ions; $LET=21.17 \text{ MeV.cm}^2/\text{mg}$ (Runs 135, 153)
4. $V_{in}=3.3V$; $V_{out}=1.5V$; $I_{out}=0.1A$; Room Temp.; Krypton Ions; $LET=30.86 \text{ MeV.cm}^2/\text{mg}$ (Runs 126)
5. $V_{in}=3.3V$; $V_{out}=1.5V$; $I_{out}=0.1A$; Room Temp.; Xenon Ions; $LET=58.78 \text{ MeV.cm}^2/\text{mg}$ (Runs 125, 154)
6. $V_{in}=5V$; $V_{out}=1.5V$; $I_{out}=0.1A$; Room Temp.; Neon Ions; $LET=3.49 \text{ MeV.cm}^2/\text{mg}$ (Runs 144, 148)
7. $V_{in}=5V$; $V_{out}=1.5V$; $I_{out}=0.1A$; Room Temp.; Argon Ions; $LET=9.74 \text{ MeV.cm}^2/\text{mg}$ (Runs 137)
8. $V_{in}=5V$; $V_{out}=1.5V$; $I_{out}=0.1A$; Room Temp.; Copper Ions; $LET=21.17 \text{ MeV.cm}^2/\text{mg}$ (Runs 134)
9. $V_{in}=5V$; $V_{out}=1.5V$; $I_{out}=0.1A$; Room Temp.; Krypton Ions; $LET=30.86 \text{ MeV.cm}^2/\text{mg}$ (Runs 127)
10. $V_{in}=5V$; $V_{out}=1.5V$; $I_{out}=0.1A$; Room Temp.; Xenon Ions; $LET=58.78 \text{ MeV.cm}^2/\text{mg}$ (Runs 124)
11. $V_{in}=10V$; $V_{out}=1.5V$; $I_{out}=0.1A$; Room Temp.; Neon Ions; $LET=3.49 \text{ MeV.cm}^2/\text{mg}$ (Runs 143,149)
12. $V_{in}=10V$; $V_{out}=1.5V$; $I_{out}=0.1A$; Room Temp.; Argon Ions; $LET=9.74 \text{ MeV.cm}^2/\text{mg}$ (Runs 138)
13. $V_{in}=10V$; $V_{out}=1.5V$; $I_{out}=0.1A$; Room Temp.; Copper Ions; $LET=21.17 \text{ MeV.cm}^2/\text{mg}$ (Runs 133, 152)
14. $V_{in}=10V$; $V_{out}=1.5V$; $I_{out}=0.1A$; Room Temp.; Krypton Ions; $LET=30.86 \text{ MeV.cm}^2/\text{mg}$ (Runs 128)
15. $V_{in}=10V$; $V_{out}=1.5V$; $I_{out}=0.1A$; Room Temp.; Xenon Ions; $LET=58.78 \text{ MeV.cm}^2/\text{mg}$ (Runs 123, 155)
16. $V_{in}=16V$; $V_{out}=1.5V$; $I_{out}=0.1A$; Room Temp.; Neon Ions; $LET=3.49 \text{ MeV.cm}^2/\text{mg}$ (Runs 142)
17. $V_{in}=16V$; $V_{out}=1.5V$; $I_{out}=0.1A$; Room Temp.; Argon Ions; $LET=9.74 \text{ MeV.cm}^2/\text{mg}$ (Runs 139)
18. $V_{in}=16V$; $V_{out}=1.5V$; $I_{out}=0.1A$; Room Temp.; Copper Ions; $LET=21.17 \text{ MeV.cm}^2/\text{mg}$ (Runs 132)
19. $V_{in}=16V$; $V_{out}=1.5V$; $I_{out}=0.1A$; Room Temp.; Krypton Ions; $LET=30.86 \text{ MeV.cm}^2/\text{mg}$ (Runs 129)
20. $V_{in}=16V$; $V_{out}=1.5V$; $I_{out}=0.1A$; Room Temp.; Xenon Ions; $LET=58.78 \text{ MeV.cm}^2/\text{mg}$ (Runs 122)
21. $V_{in}=26V$; $V_{out}=1.5V$; $I_{out}=0.1A$; Room Temp.; Neon Ions; $LET=3.49 \text{ MeV.cm}^2/\text{mg}$ (Runs 141, 150)
22. $V_{in}=26V$; $V_{out}=1.5V$; $I_{out}=0.1A$; Room Temp.; Argon Ions; $LET=9.74 \text{ MeV.cm}^2/\text{mg}$ (Runs 140)
23. $V_{in}=26V$; $V_{out}=1.5V$; $I_{out}=0.1A$; Room Temp.; Copper Ions; $LET=21.17 \text{ MeV.cm}^2/\text{mg}$ (Runs 131, 151)
24. $V_{in}=26V$; $V_{out}=1.5V$; $I_{out}=0.1A$; Room Temp.; Krypton Ions; $LET=30.86 \text{ MeV.cm}^2/\text{mg}$ (Runs 130)
25. $V_{in}=26V$; $V_{out}=1.5V$; $I_{out}=0.1A$; Room Temp.; Xenon Ions; $LET=58.78 \text{ MeV.cm}^2/\text{mg}$ (Runs 121, 156)

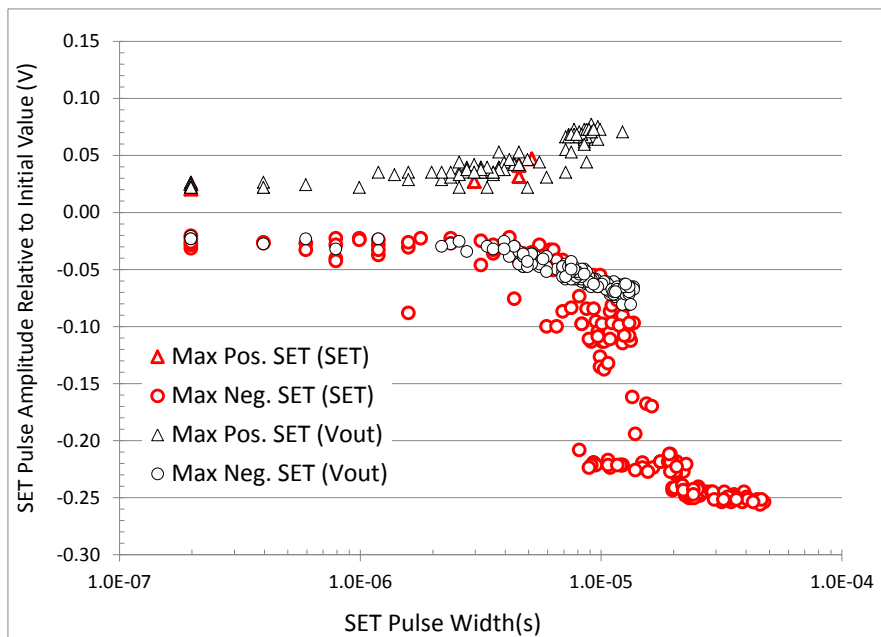
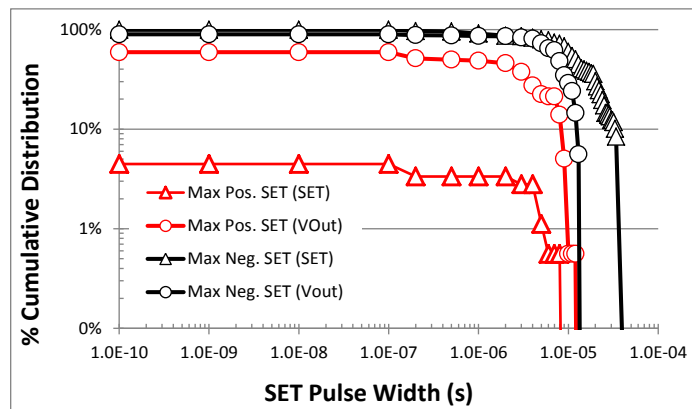
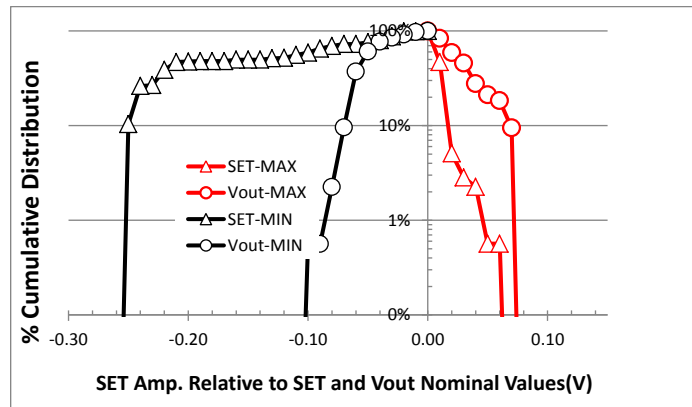
1. Vin=3.3V; Vout=1.5V; Iout=0.1A; Room Temp.; Neon Ions; LET=3.49 MeV.cm²/mg (Runs 145, 147)



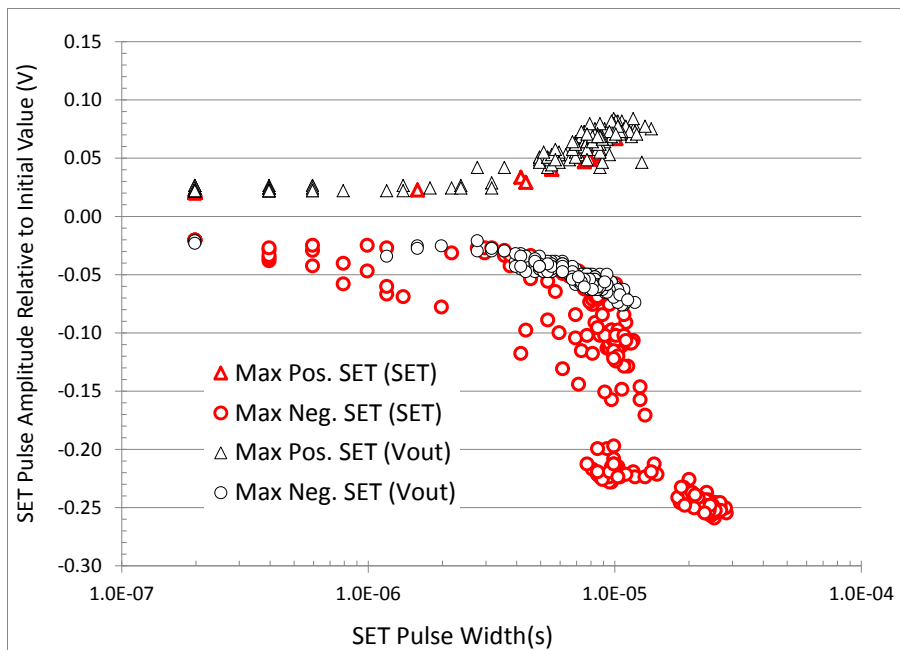
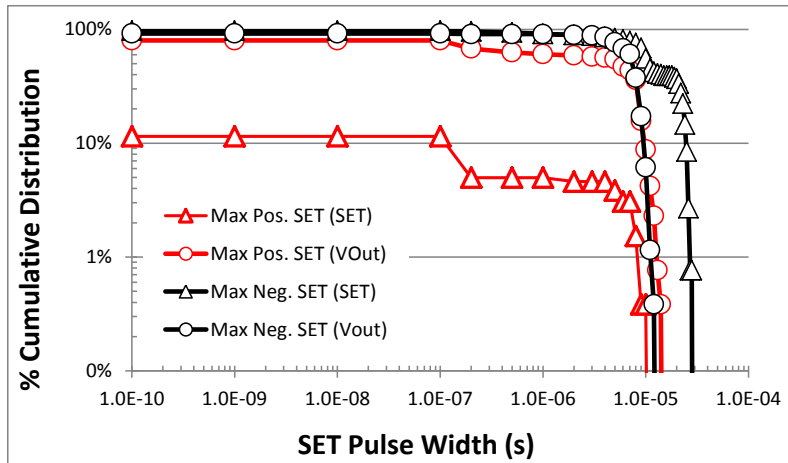
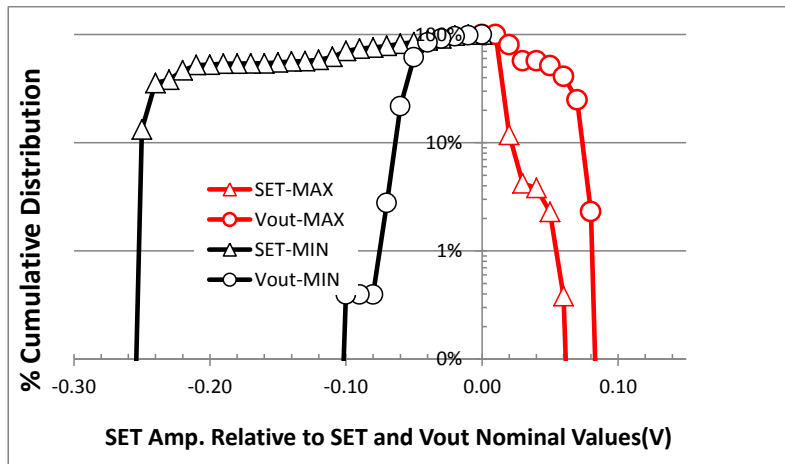
2. $V_{in}=3.3V$; $V_{out}=1.5V$; $I_{out}=0.1A$; Room Temp.; Argon Ions; $LET=9.74 \text{ MeV}\cdot\text{cm}^2/\text{mg}$ (Runs 136)



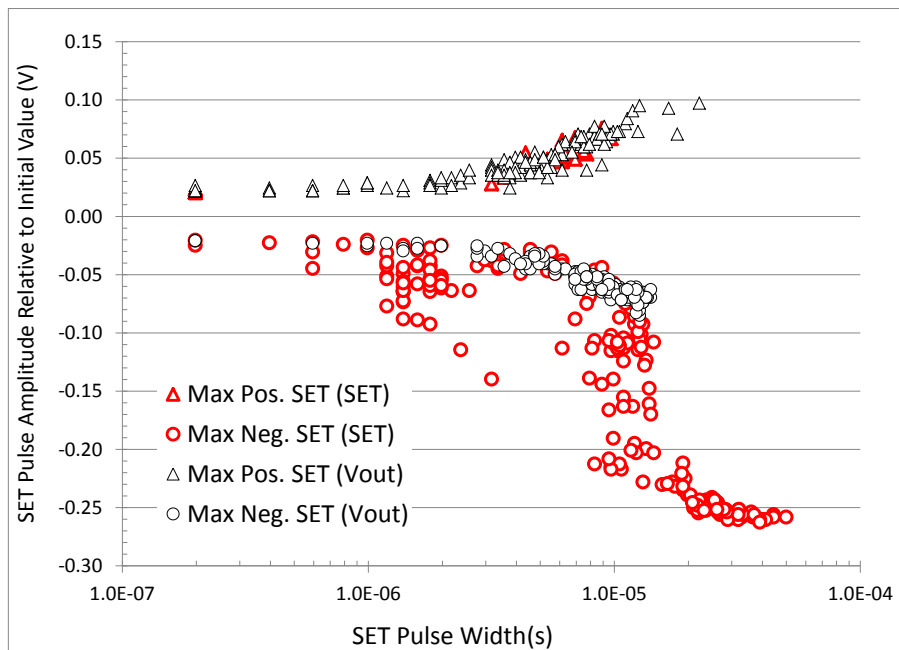
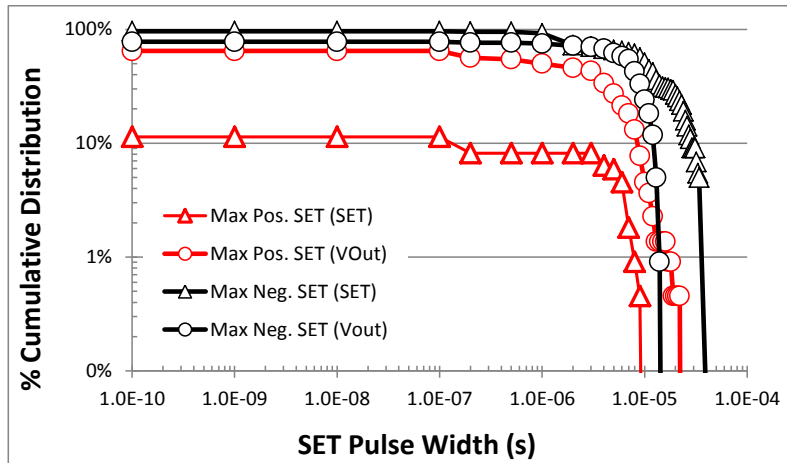
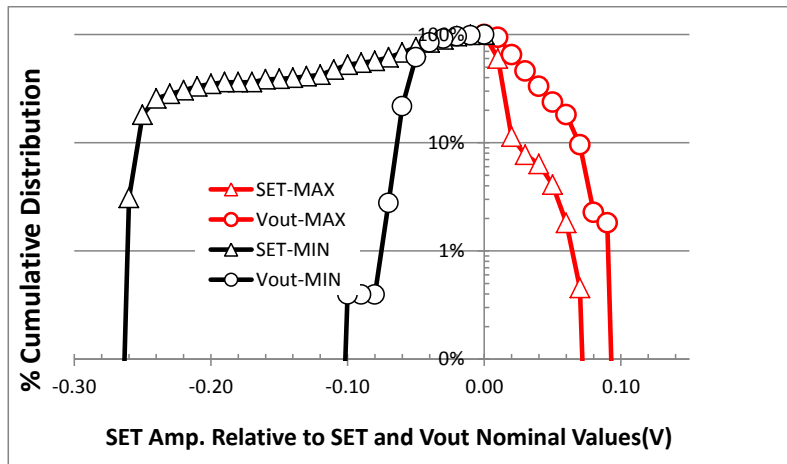
3. $V_{in}=3.3V$; $V_{out}=1.5V$; $I_{out}=0.1A$; Room Temp.; Copper Ions; $LET=21.17 \text{ MeV}\cdot\text{cm}^2/\text{mg}$ (Runs 135, 153)



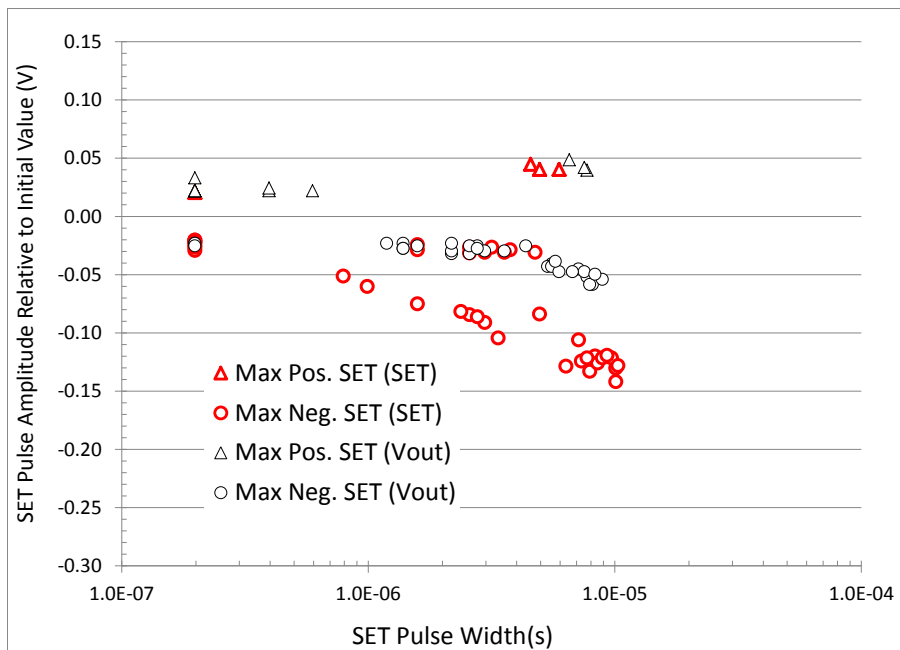
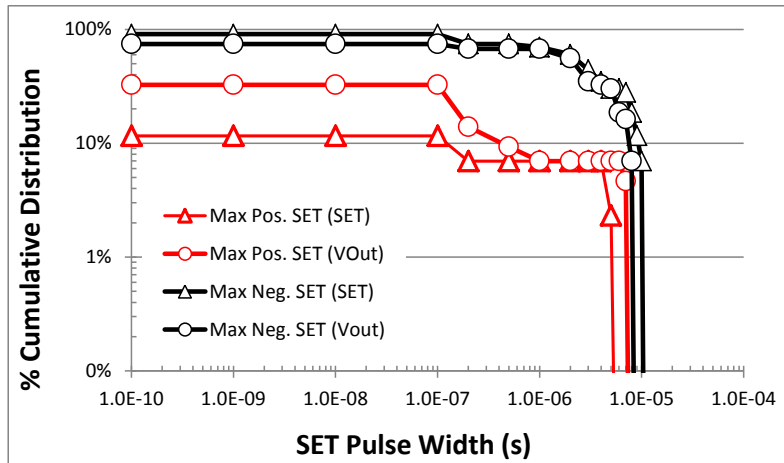
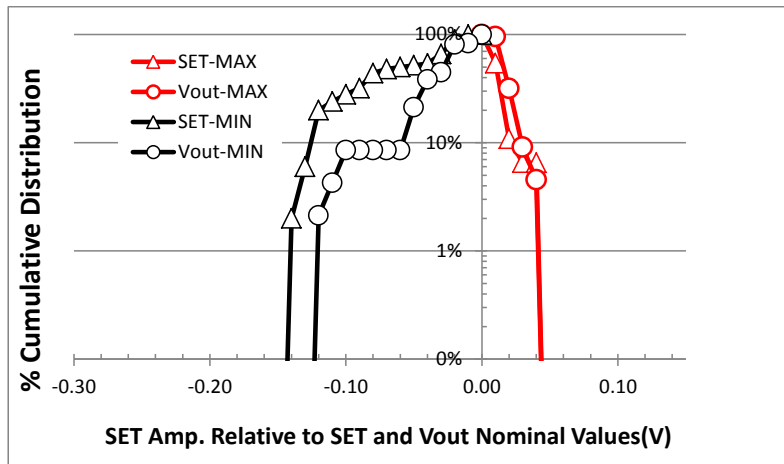
4. $V_{in}=3.3V$; $V_{out}=1.5V$; $I_{out}=0.1A$; Room Temp.; Krypton Ions; LET=30.86 MeV.cm²/mg (Runs 126)



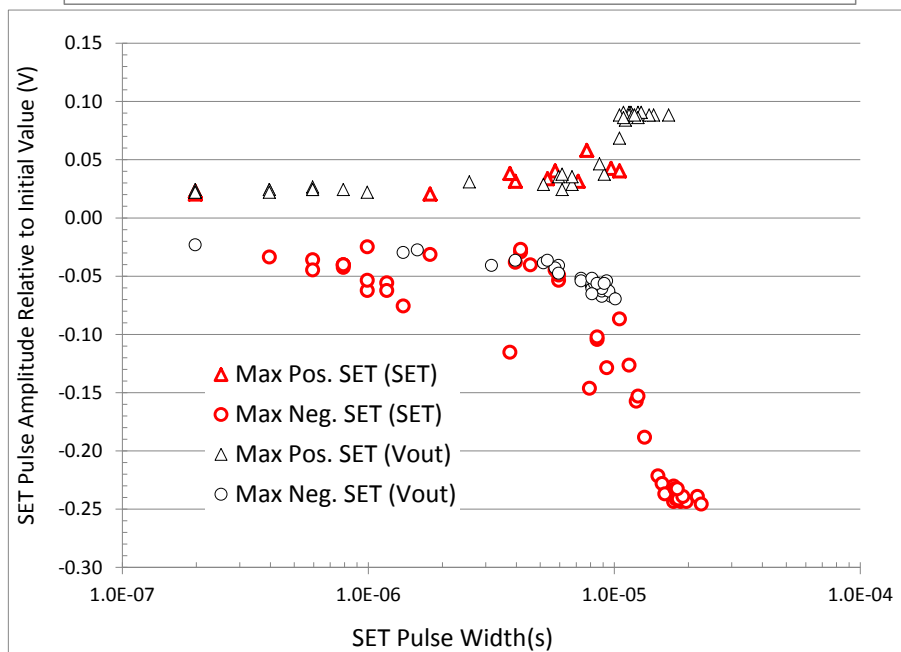
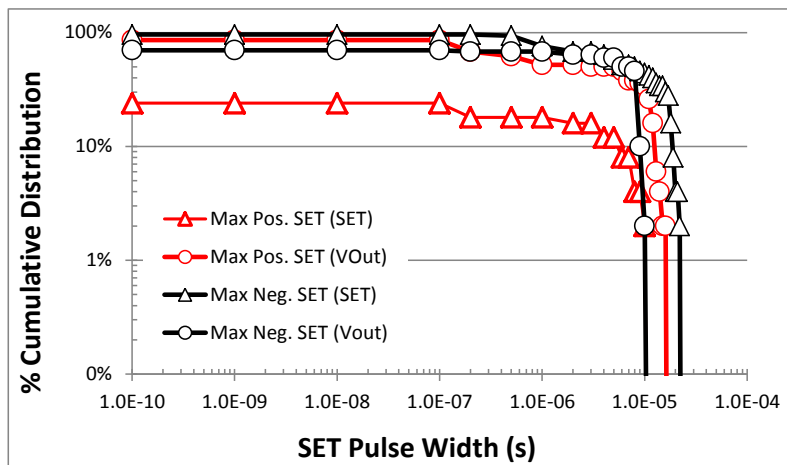
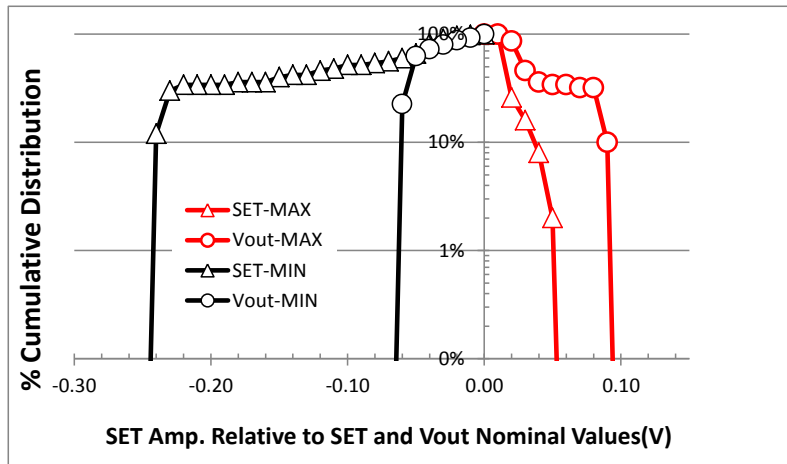
5. $V_{in}=3.3V$; $V_{out}=1.5V$; $I_{out}=0.1A$; Room Temp.; Xenon Ions; LET=58.78 MeV.cm²/mg (Runs 125, 154)



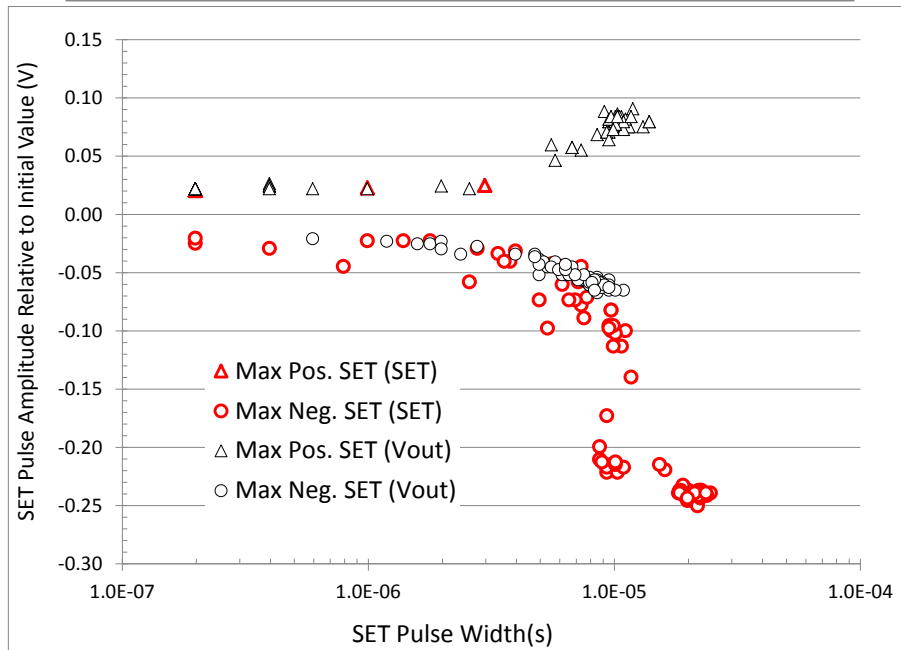
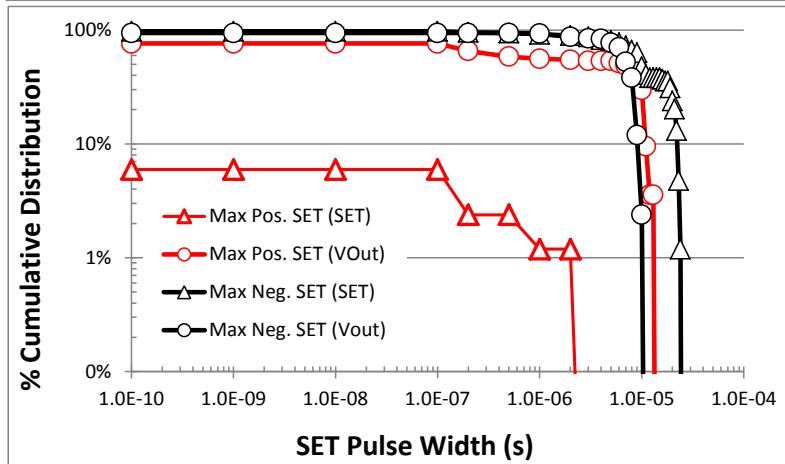
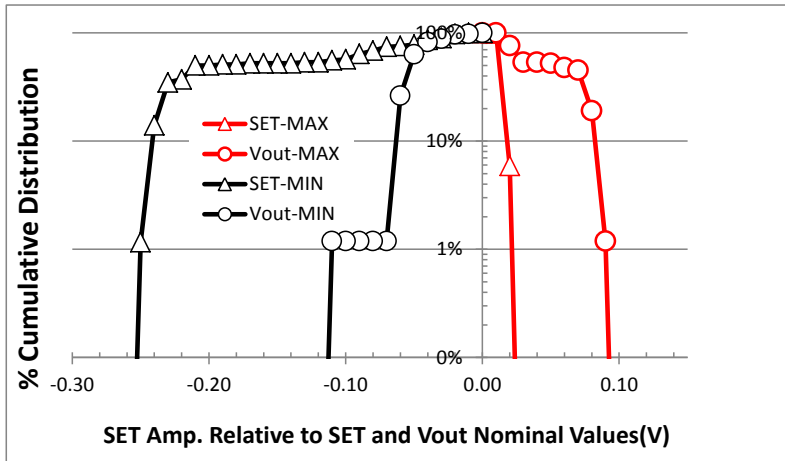
6. $V_{in}=5V$; $V_{out}=1.5V$; $I_{out}=0.1A$; Room Temp.; Neon Ions; $LET=3.49 \text{ MeV}\cdot\text{cm}^2/\text{mg}$ (Runs 144, 148)



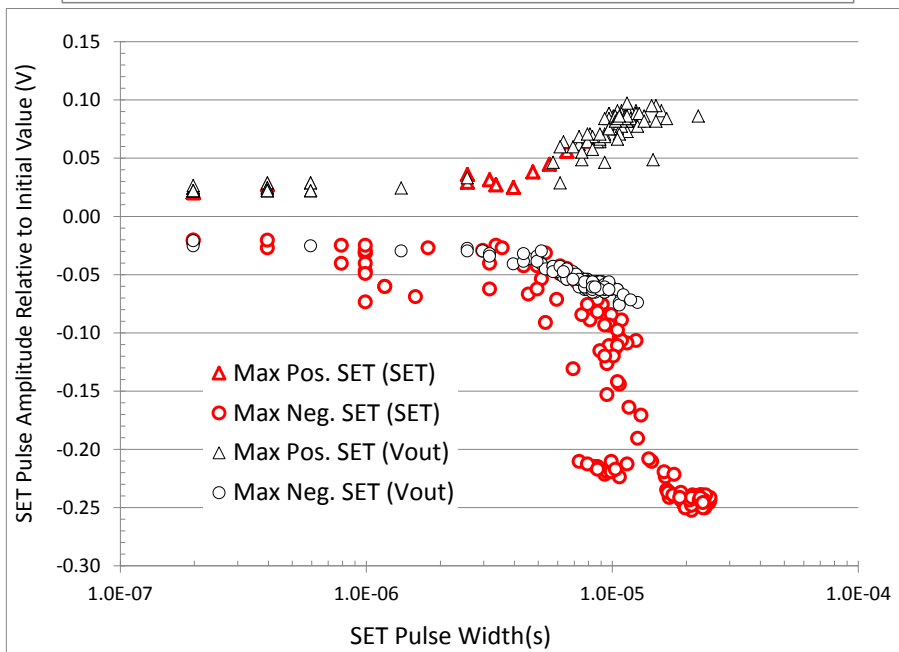
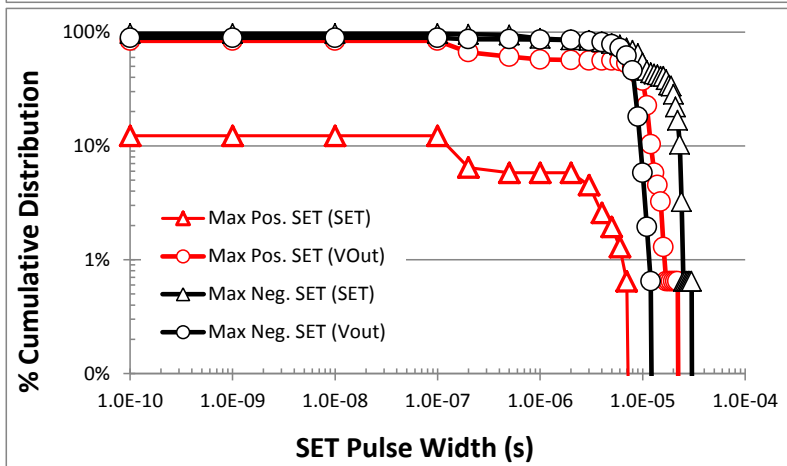
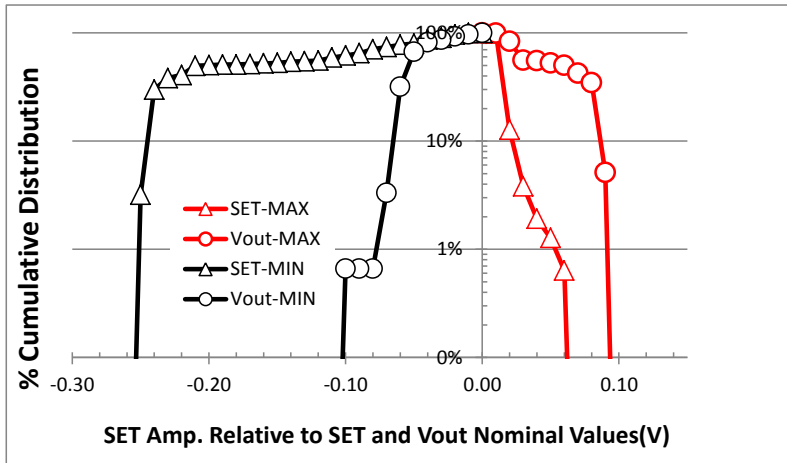
7. $V_{in}=5V$; $V_{out}=1.5V$; $I_{out}=0.1A$; Room Temp.; Argon Ions; LET=9.74 MeV.cm²/mg (Runs 137)



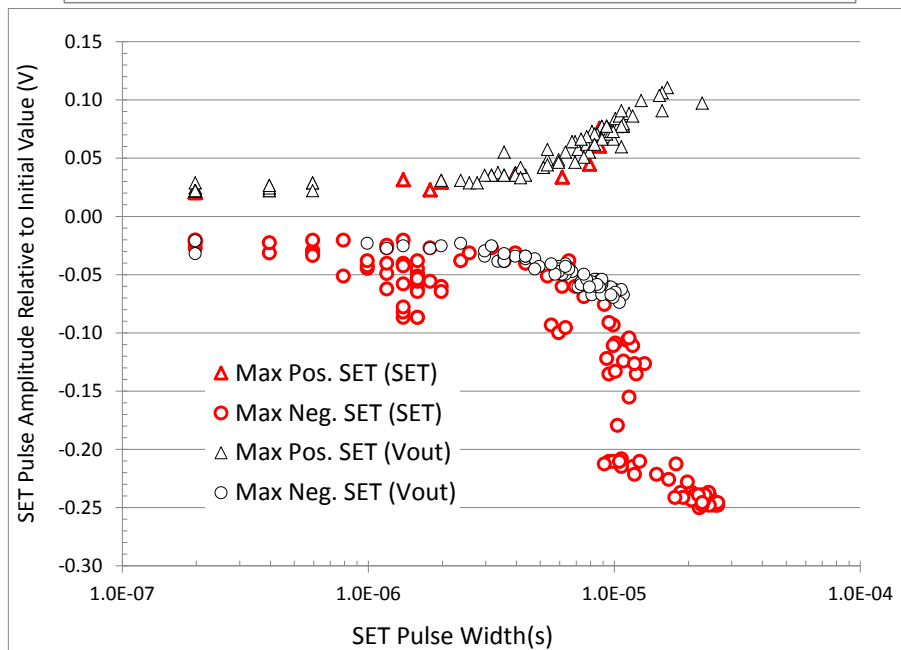
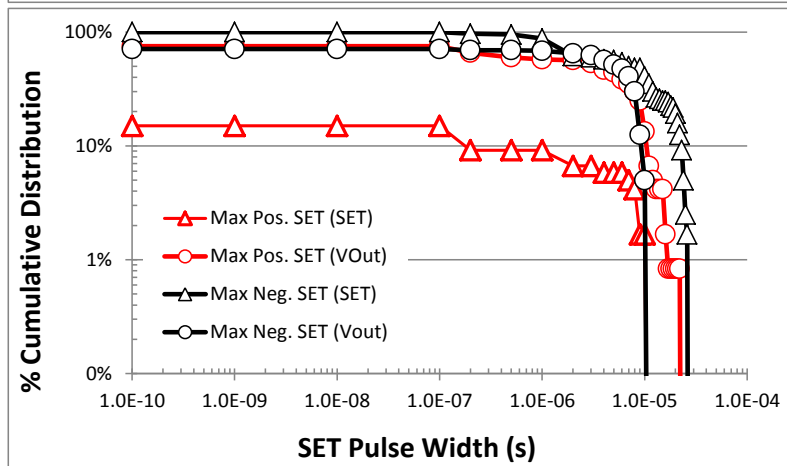
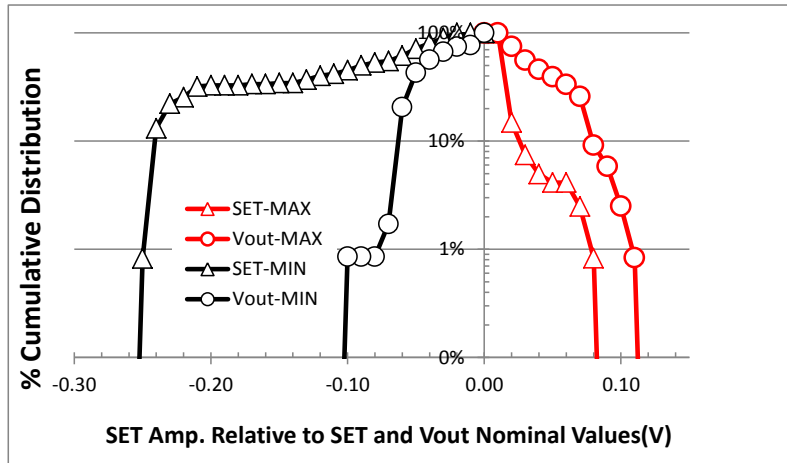
8. $V_{in}=5V$; $V_{out}=1.5V$; $I_{out}=0.1A$; Room Temp.; Copper Ions; LET=21.17 MeV.cm²/mg (Runs 134)



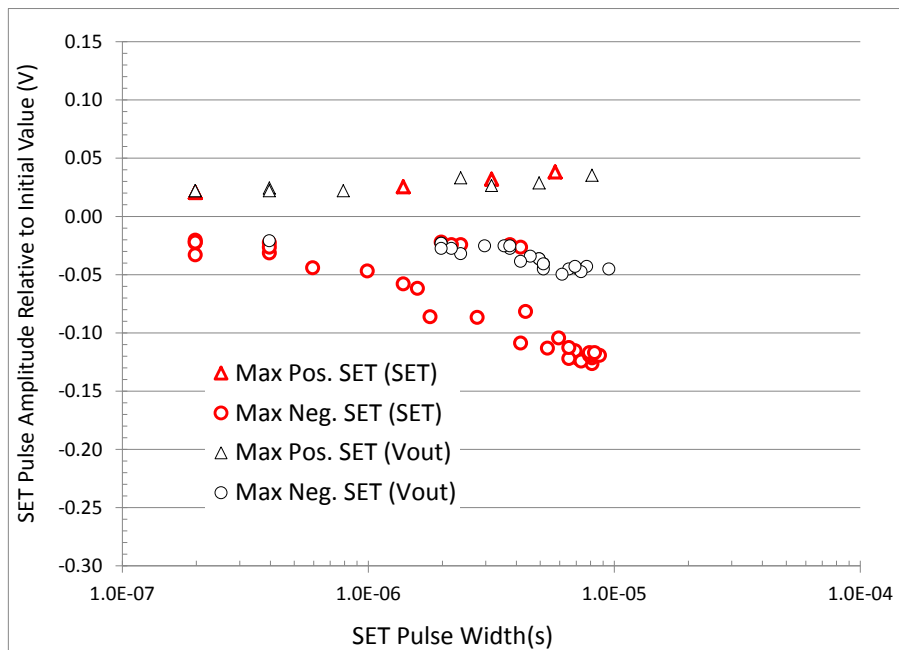
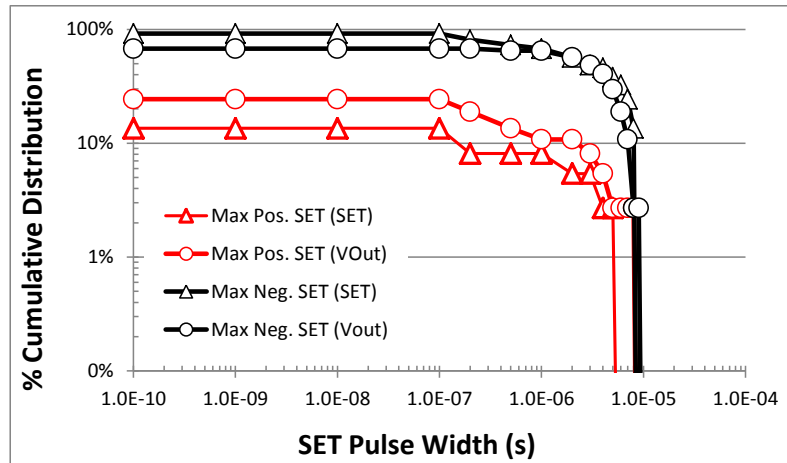
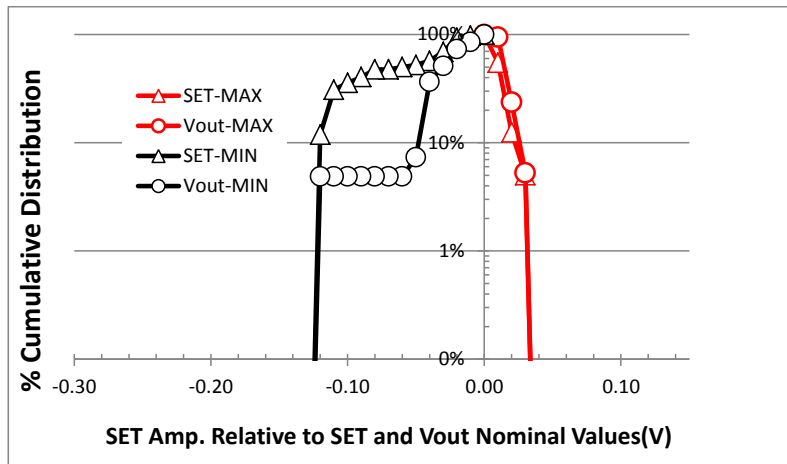
9. $V_{in}=5V$; $V_{out}=1.5V$; $I_{out}=0.1A$; Room Temp.; Krypton Ions; LET=30.86 MeV.cm²/mg (Runs 127)



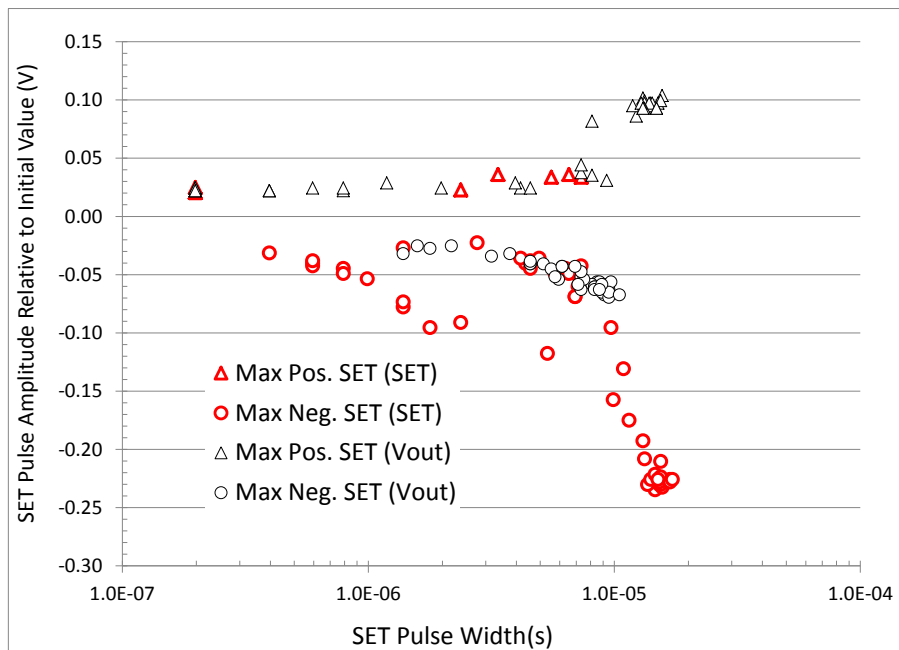
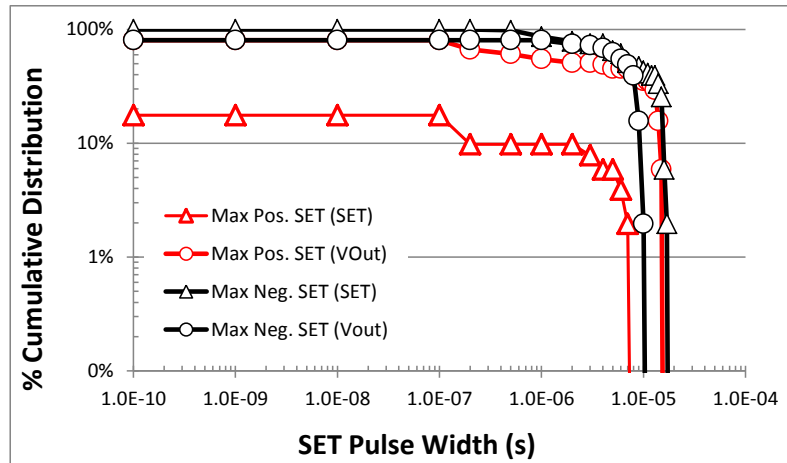
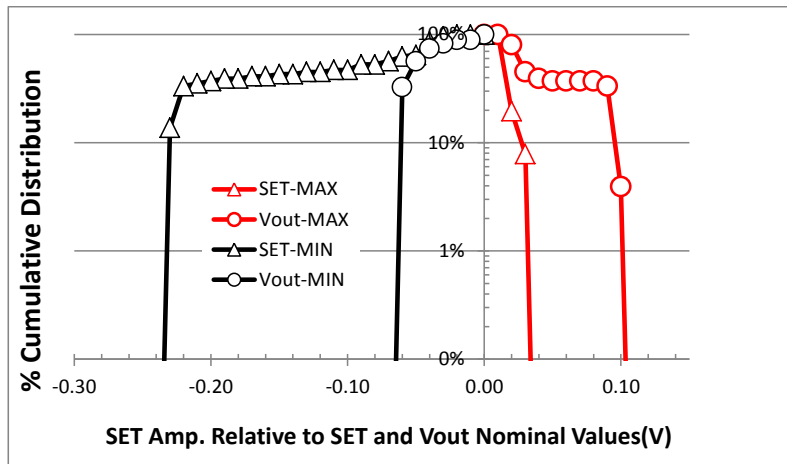
10. $V_{in}=5V$; $V_{out}=1.5V$; $I_{out}=0.1A$; Room Temp.; Xenon Ions; LET=58.78 MeV.cm²/mg (Runs 124)



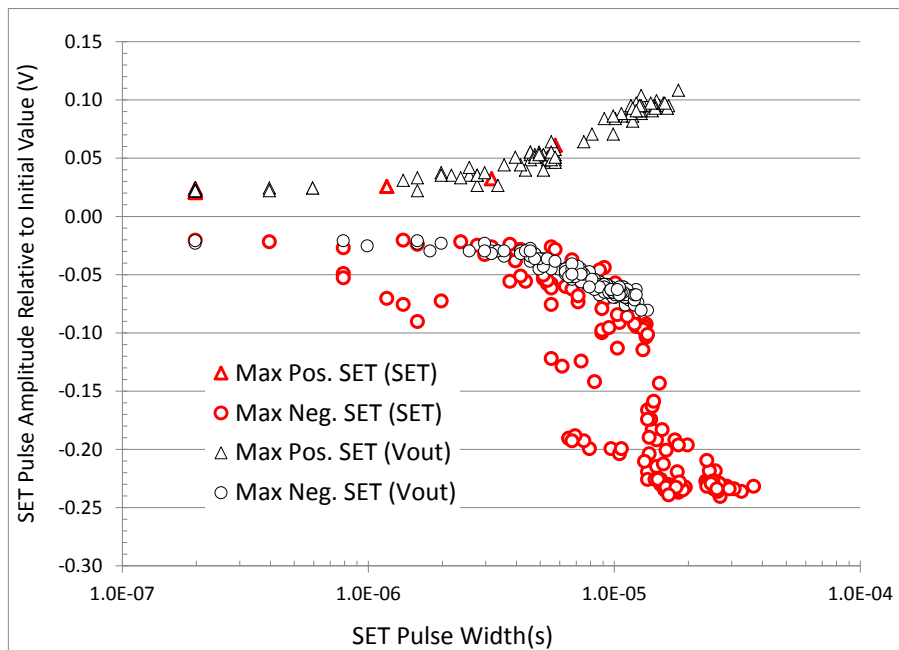
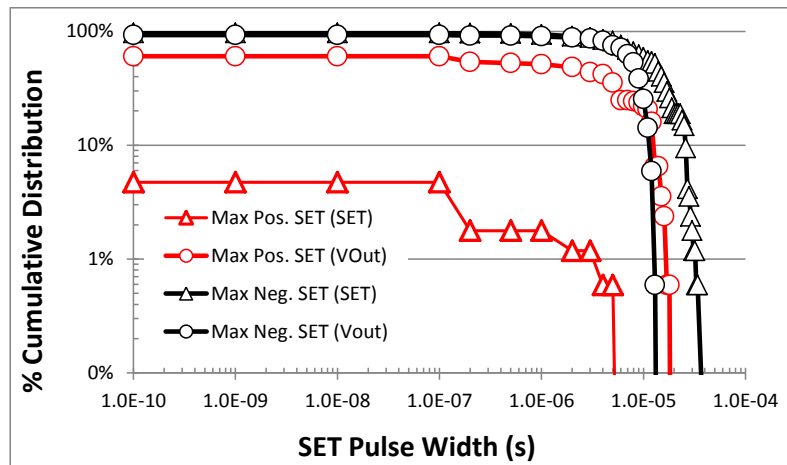
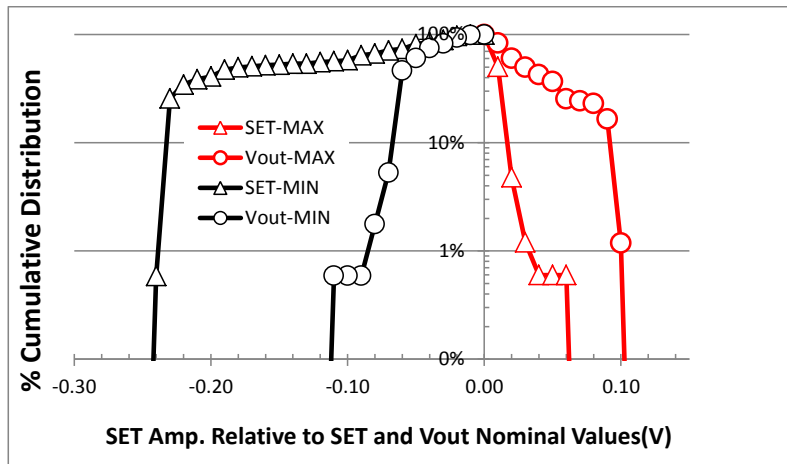
11. $V_{in}=10V$; $V_{out}=1.5V$; $I_{out}=0.1A$; Room Temp.; Neon Ions; LET=3.49 MeV.cm²/mg (Runs 143,149)



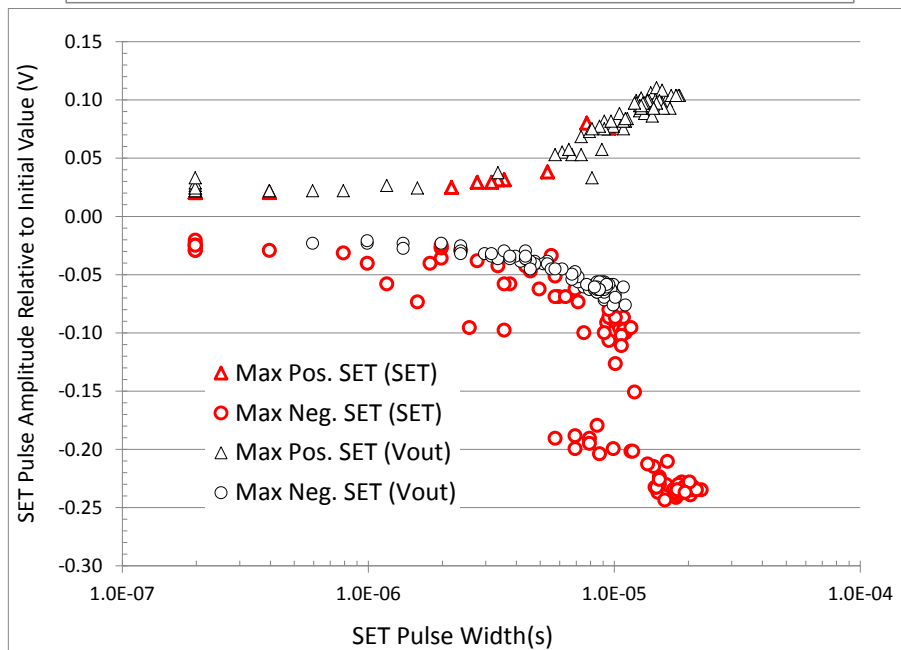
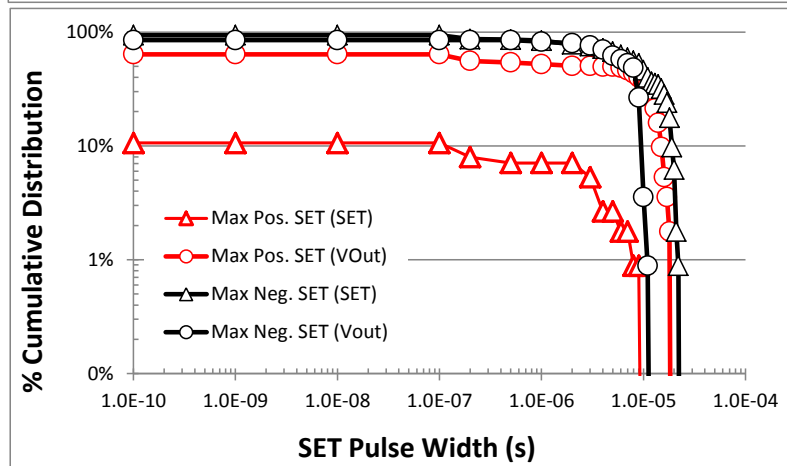
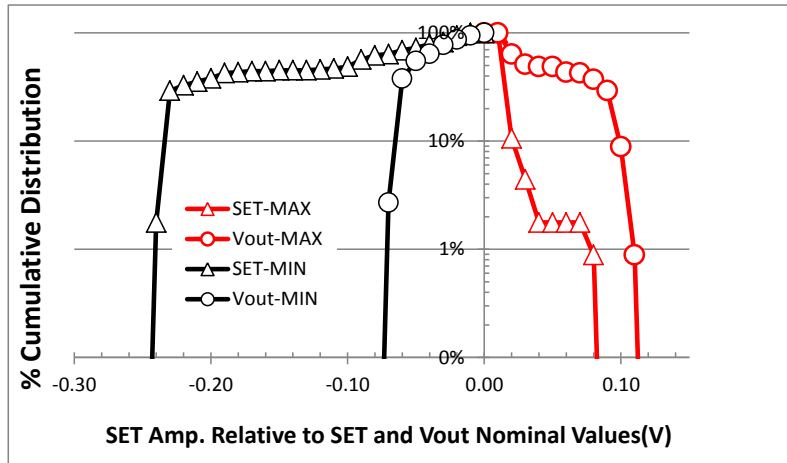
12. $V_{in}=10V$; $V_{out}=1.5V$; $I_{out}=0.1A$; Room Temp.; Argon Ions; $LET=9.74 \text{ MeV.cm}^2/\text{mg}$ (Runs 138)



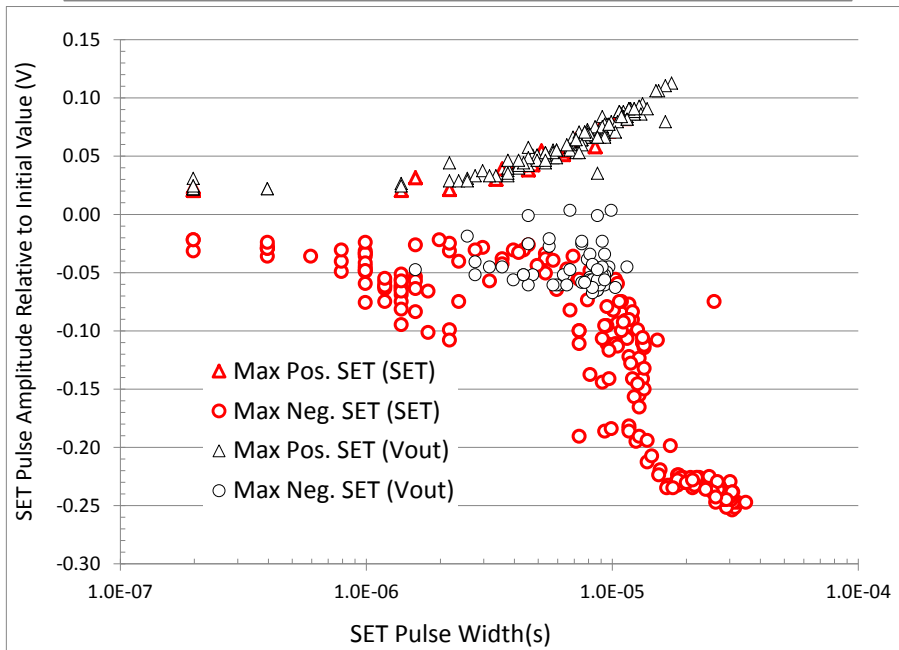
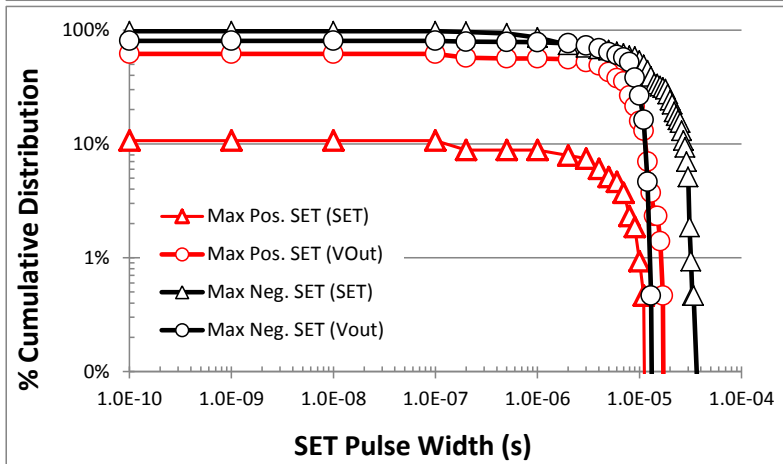
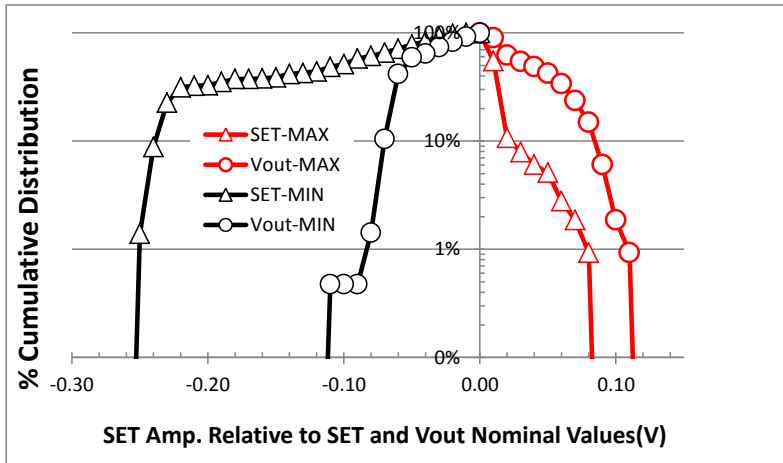
13. $V_{in}=10V$; $V_{out}=1.5V$; $I_{out}=0.1A$; Room Temp.; Copper Ions; $LET=21.17 \text{ MeV}\cdot\text{cm}^2/\text{mg}$ (Runs 133, 152)



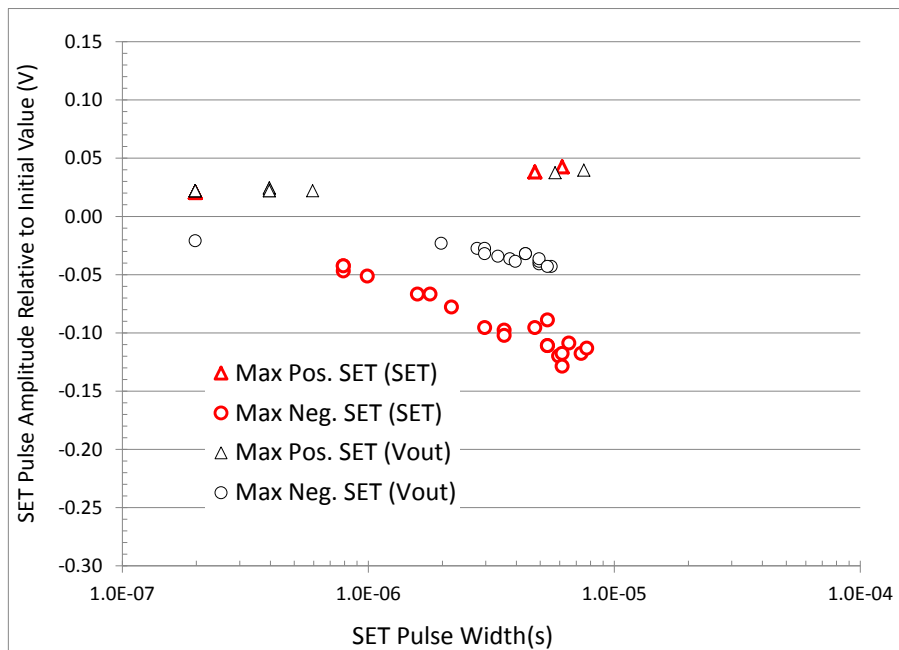
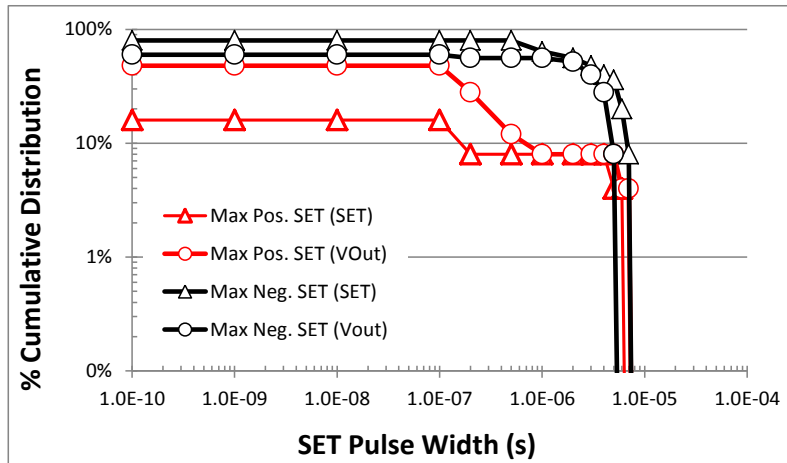
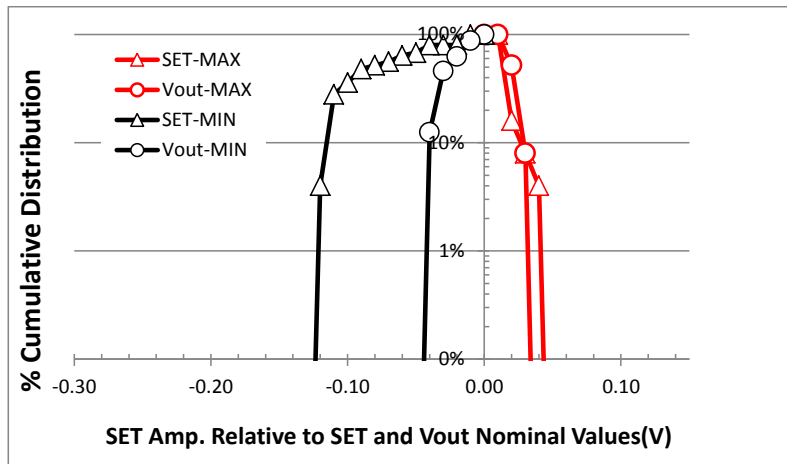
14. $V_{in}=10V$; $V_{out}=1.5V$; $I_{out}=0.1A$; Room Temp.; Krypton Ions; $LET=30.86 \text{ MeV}\cdot\text{cm}^2/\text{mg}$ (Runs 128)



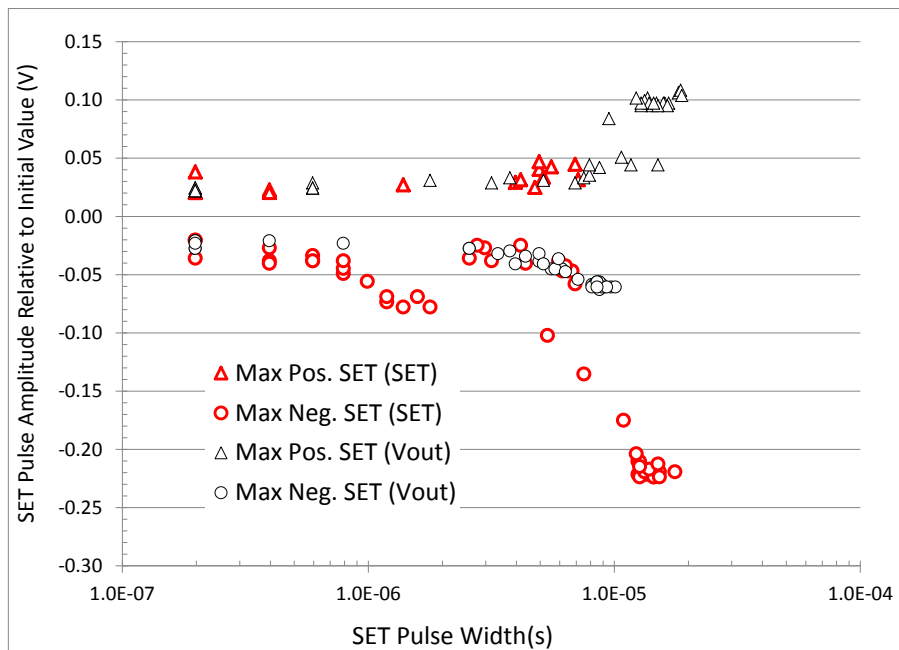
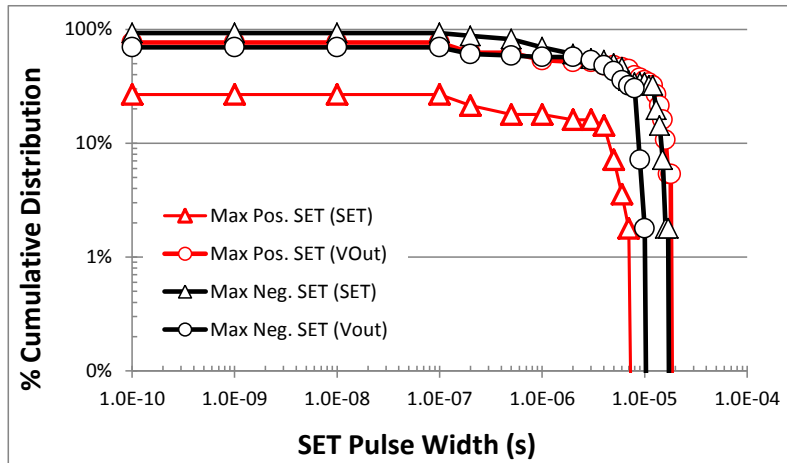
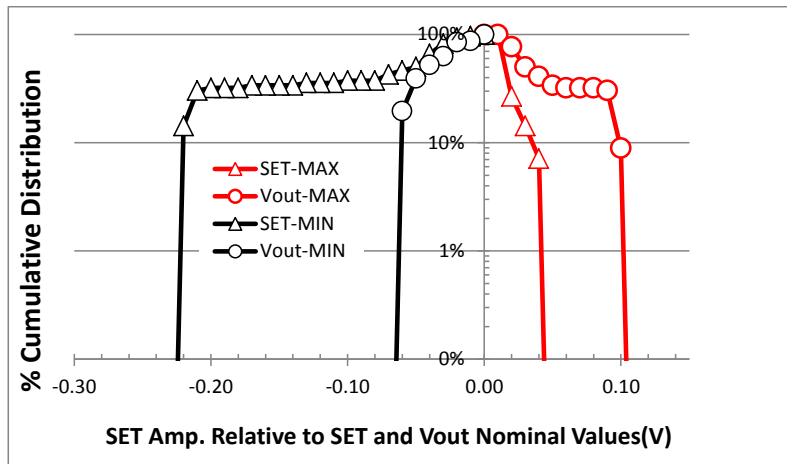
15. $V_{in}=10V$; $V_{out}=1.5V$; $I_{out}=0.1A$; Room Temp.; Xenon Ions; $LET=58.78 \text{ MeV}\cdot\text{cm}^2/\text{mg}$ (Runs 123, 155)



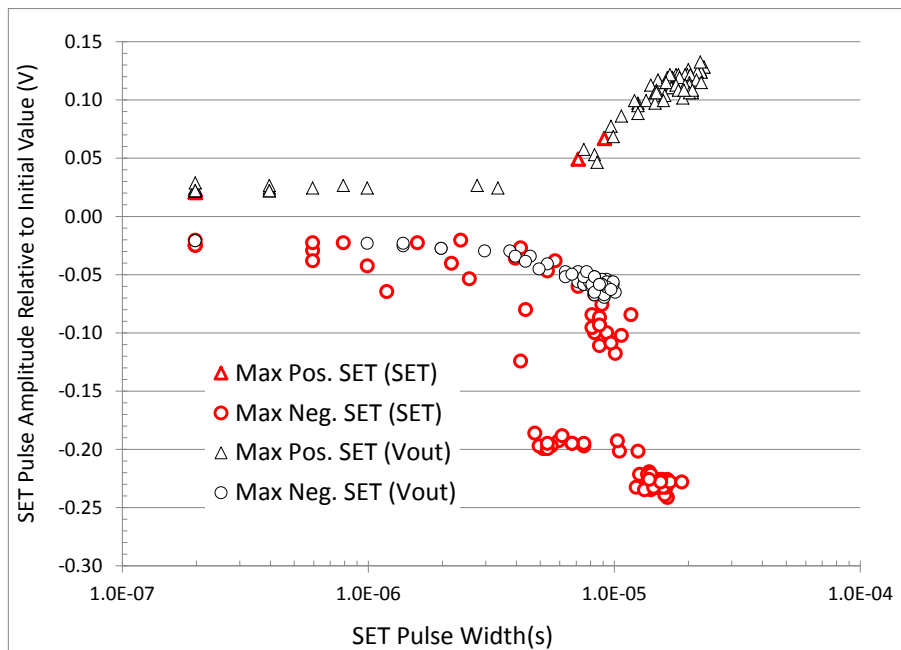
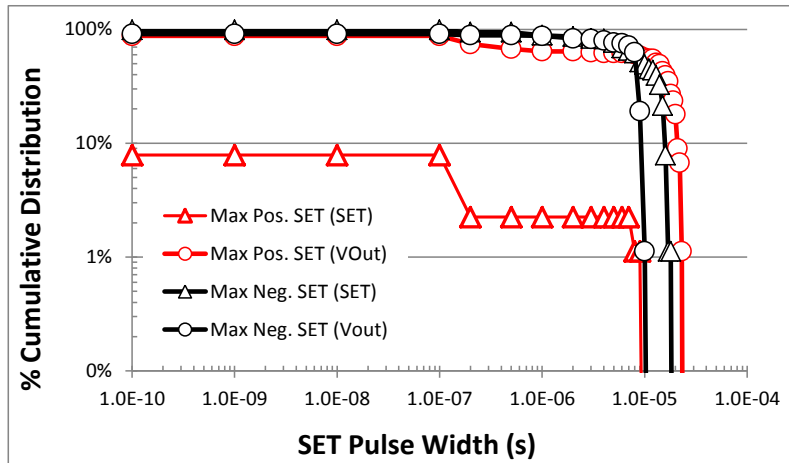
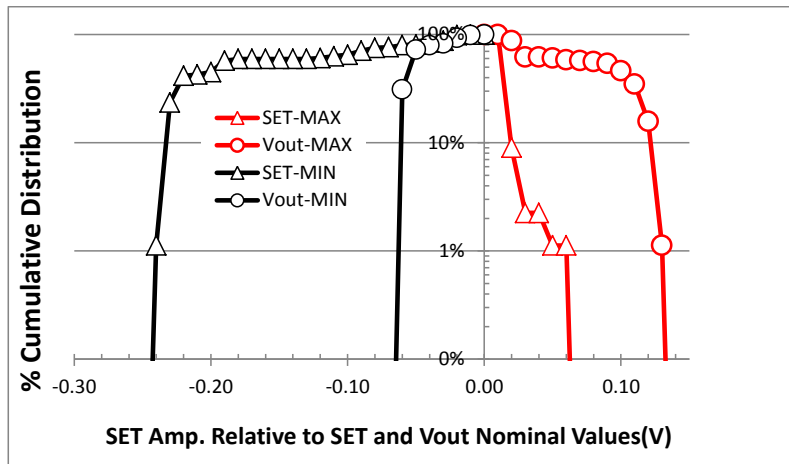
16. $V_{in}=16V$; $V_{out}=1.5V$; $I_{out}=0.1A$; Room Temp.; Neon Ions; LET=3.49 MeV.cm²/mg (Runs 142)



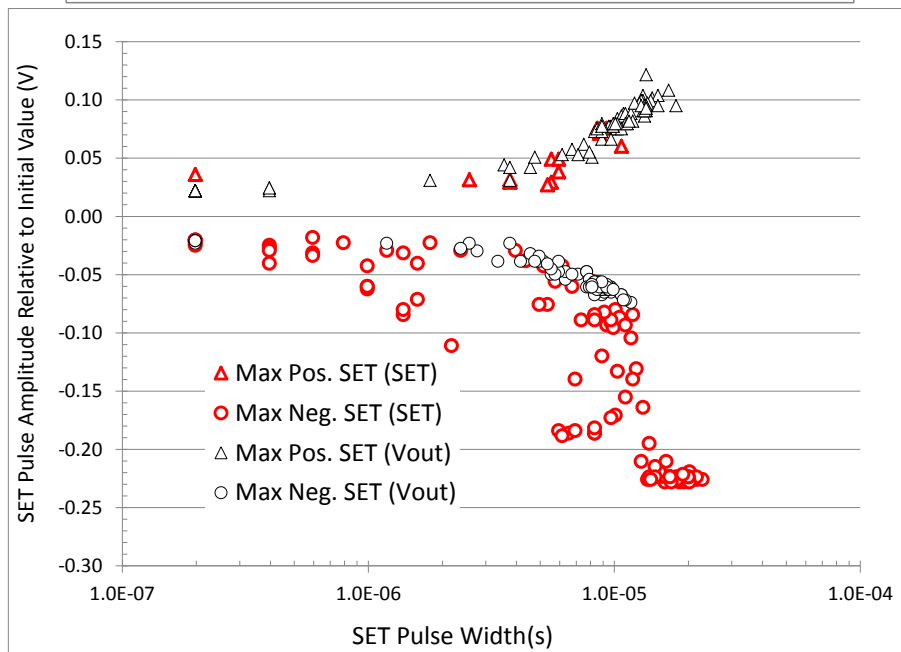
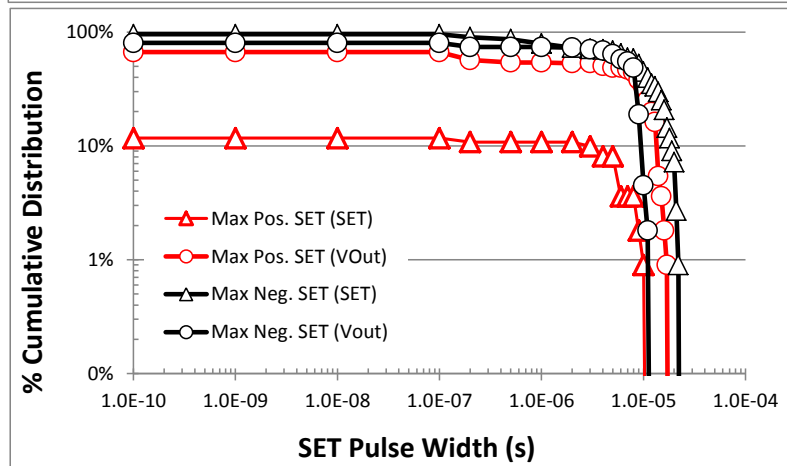
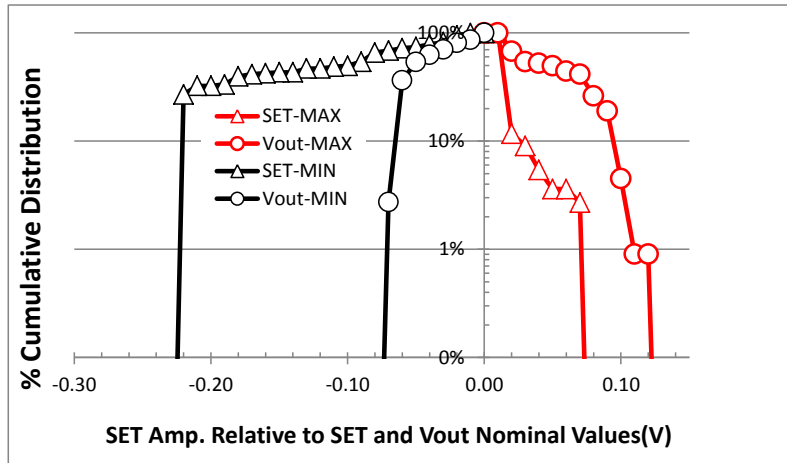
17. $V_{in}=16V$; $V_{out}=1.5V$; $I_{out}=0.1A$; Room Temp.; Argon Ions; LET=9.74 MeV.cm²/mg (Runs 139)



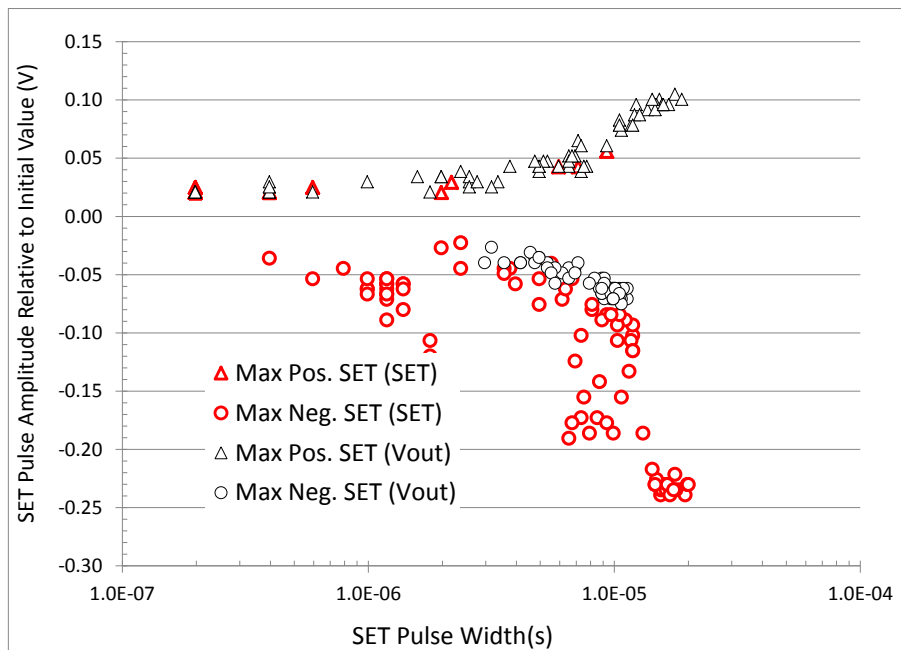
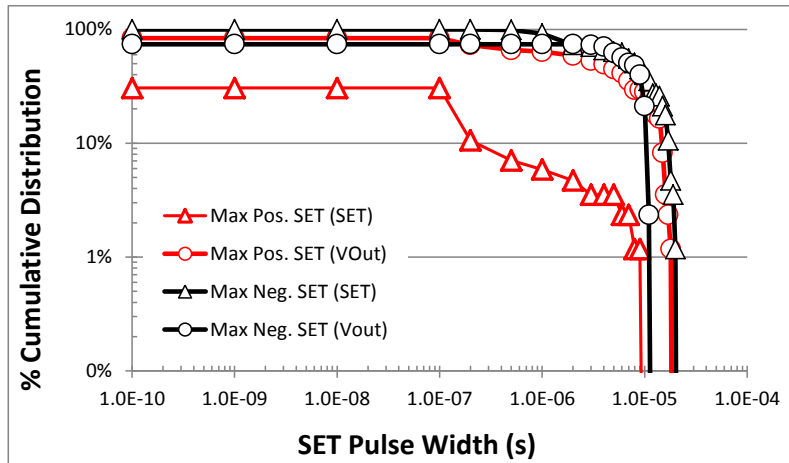
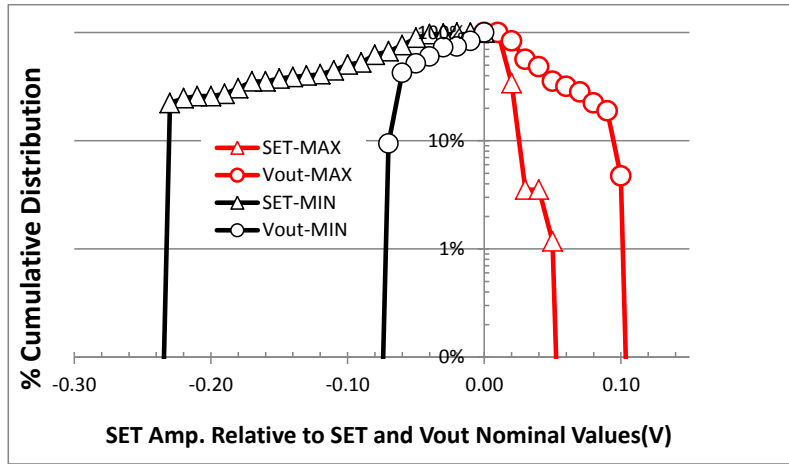
18. $V_{in}=16V$; $V_{out}=1.5V$; $I_{out}=0.1A$; Room Temp.; Copper Ions; LET=21.17 MeV.cm²/mg (Runs 132)



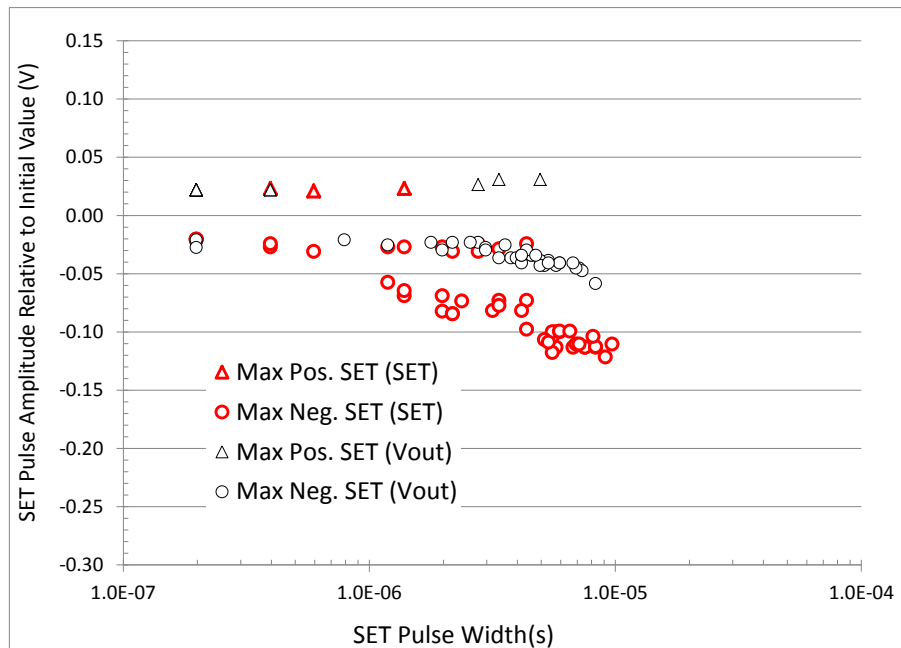
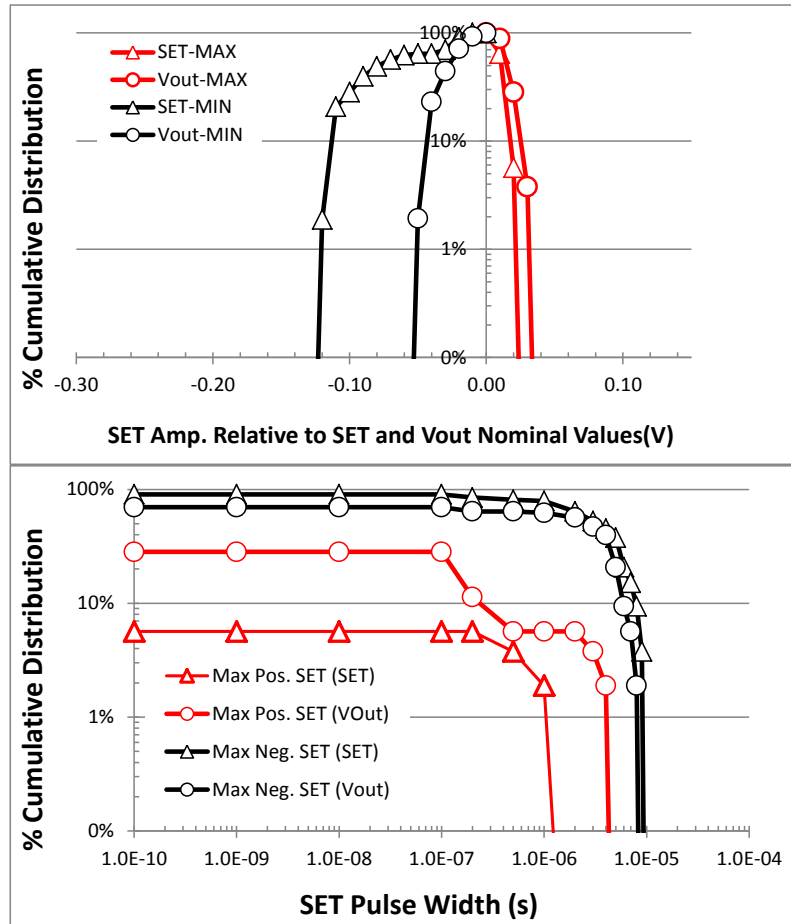
19. $V_{in}=16V$; $V_{out}=1.5V$; $I_{out}=0.1A$; Room Temp.; Krypton Ions; LET=30.86 MeV.cm²/mg (Runs 129)



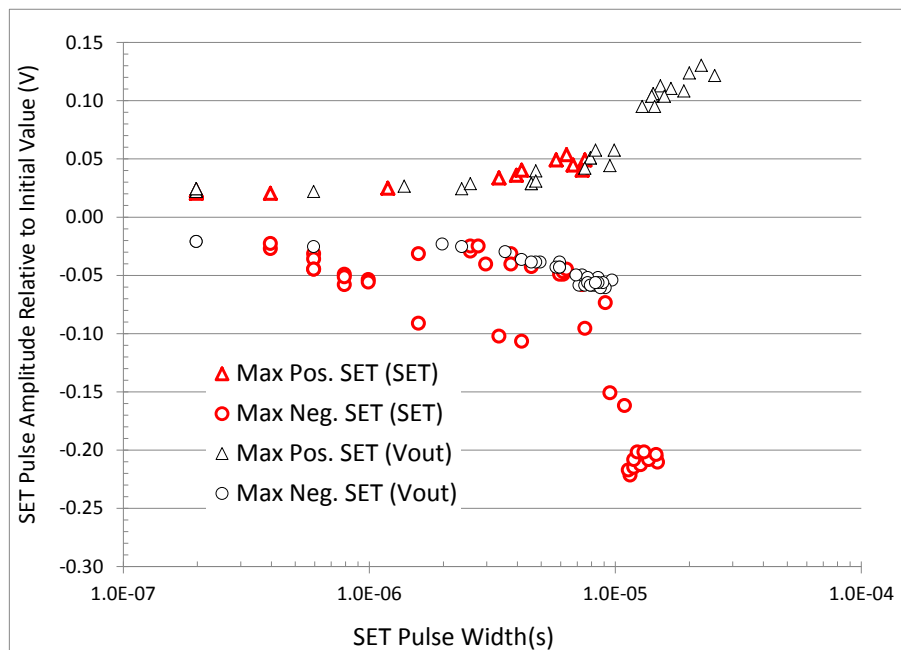
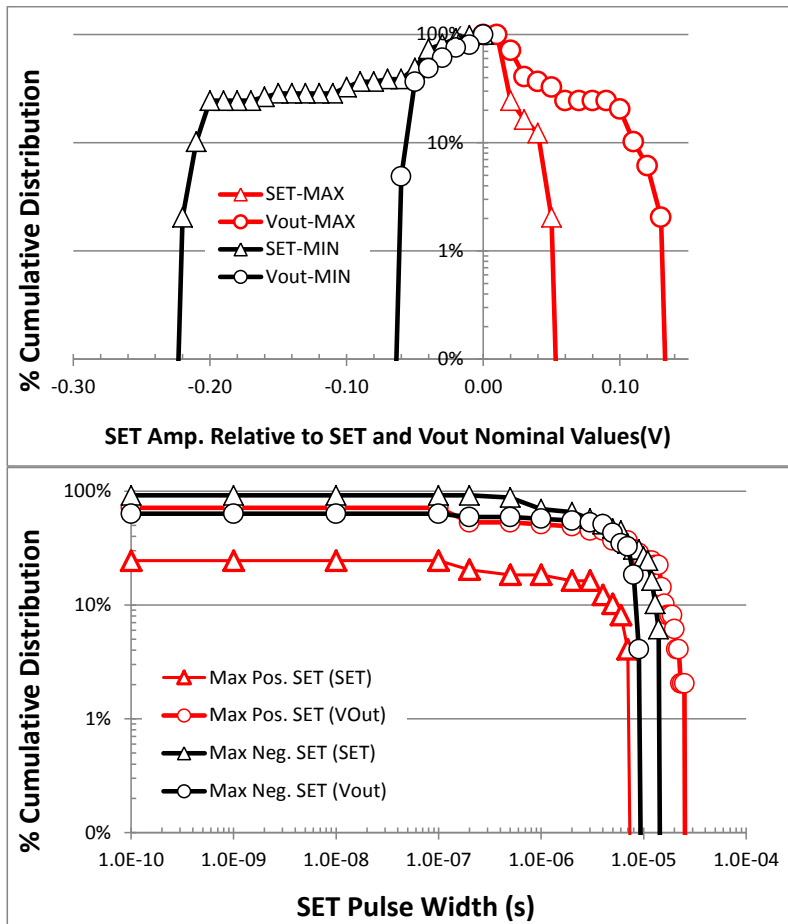
20. $V_{in}=16V$; $V_{out}=1.5V$; $I_{out}=0.1A$; Room Temp.; Xenon Ions; LET=58.78 MeV.cm²/mg (Runs 122)



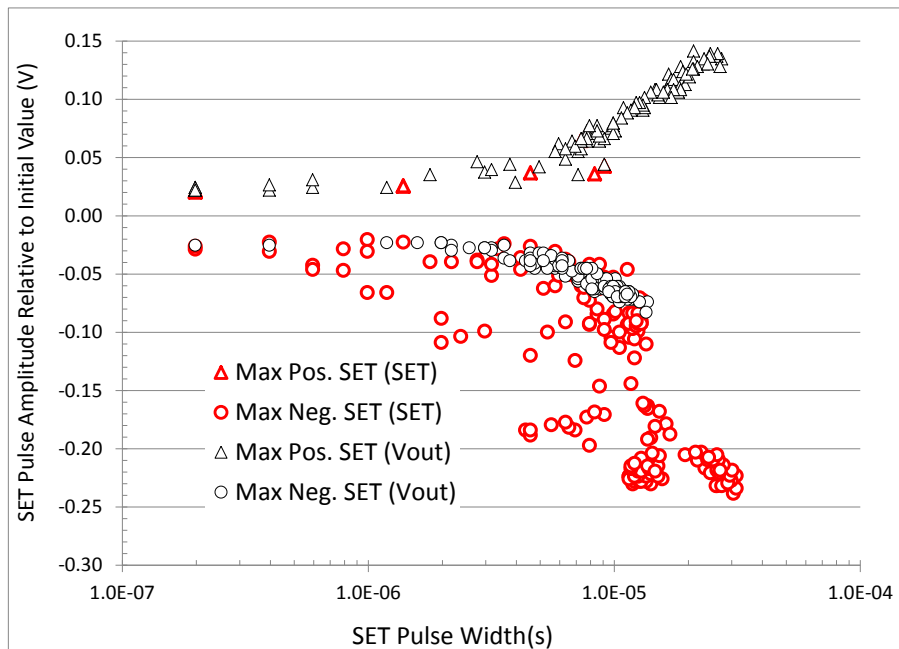
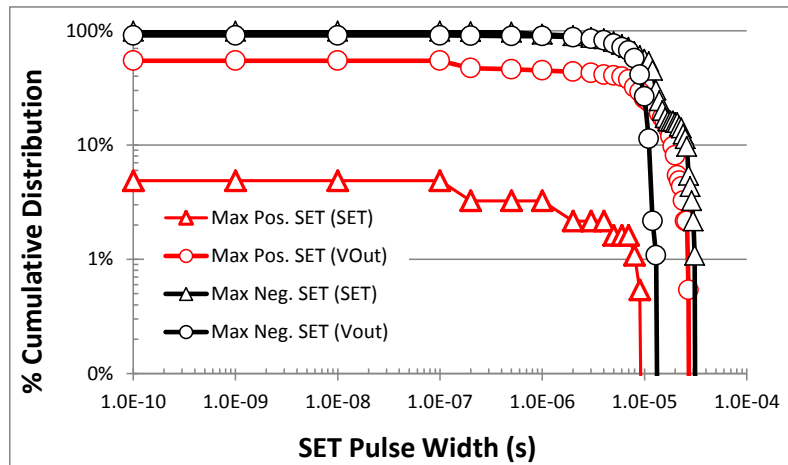
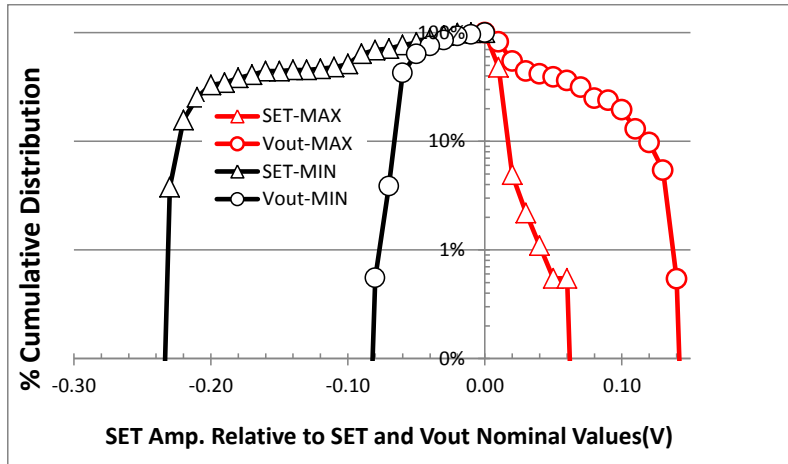
21. $V_{in}=26V$; $V_{out}=1.5V$; $I_{out}=0.1A$; Room Temp.; Neon Ions; $LET=3.49 \text{ MeV}\cdot\text{cm}^2/\text{mg}$ (Runs 141, 150)



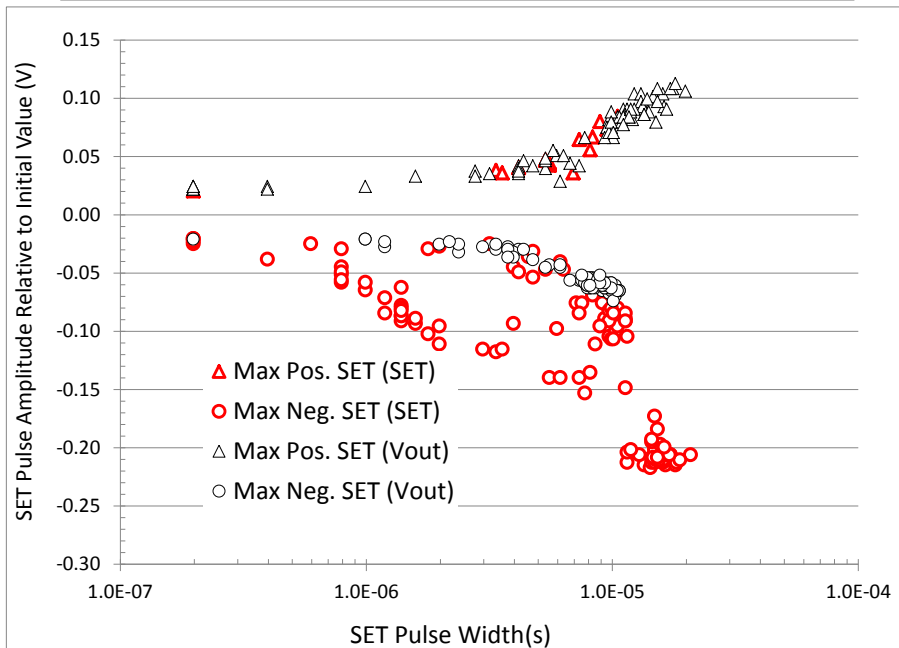
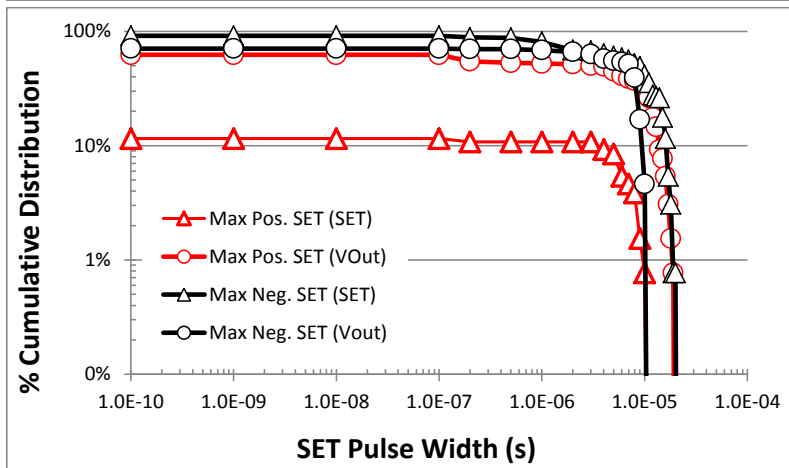
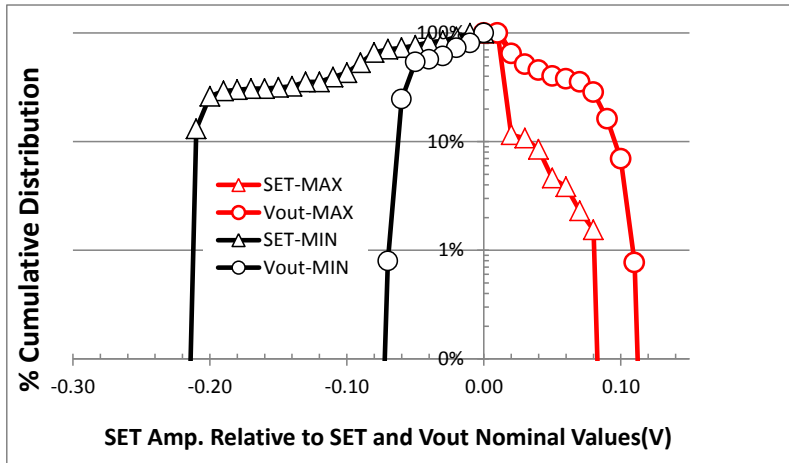
22. $V_{in}=26V$; $V_{out}=1.5V$; $I_{out}=0.1A$; Room Temp.; Argon Ions; LET=9.74 MeV.cm²/mg (Runs 140)



23. $V_{in}=26V$; $V_{out}=1.5V$; $I_{out}=0.1A$; Room Temp.; Copper Ions; $LET=21.17 \text{ MeV}\cdot\text{cm}^2/\text{mg}$ (Runs 131, 151)



24. $V_{in}=26V$; $V_{out}=1.5V$; $I_{out}=0.1A$; Room Temp.; Krypton Ions; LET=30.86 MeV.cm²/mg (Runs 130)



25. $V_{in}=26V$; $V_{out}=1.5V$; $I_{out}=0.1A$; Room Temp.; Xenon Ions; LET=58.78 MeV.cm²/mg (Runs 121, 156)

